https://doi.org/10.5194/egusphere-2026-2315
Preprint. Discussion started: 20 May 2026

Past and future evolution of cut-off-low-associated extreme precipitation in Europe

Josip Brajkovic[1], Pierre Archambeau[3], Nicolas Ghilain[1,2], and Sébastien Doutreloup[1]

[1]Laboratory of Climatology, Department of Geography, SPHERES research unit, University of Liège, Liège, Belgium.
[2]Royal Meteorological Institute, RMI, Uccle, Belgium
[3]Department of Environmental Engineering, University of Liege, Liege, Belgium

Correspondence: Josip Brajkovic (josip.brajkovic@uliege.be)

Abstract.

Extreme precipitation events are projected to become more frequent and intense in Europe under climate change. In recent decades, cut-off lows (COLs)—cold-core, upper-level low-pressure systems originating from polar regions—have caused severe impacts across several European countries, leading to unprecedented rainfall totals. Understanding how the influence of COLs on extreme precipitation may evolve in a warming climate is therefore a key scientific challenge. To address this issue, we develop an objective detection algorithm based on 500 hPa geopotential height (Z500) fields to identify COLs.

Using the ERA5 reanalysis for both daily precipitation and Z500 fields, we construct a climatology of COLs affecting Europe over the period 1940–2024. We first show that the total number of COLs exhibits no significant long-term trend. We then attribute daily precipitation events to potential COL influence. Our results indicate that approximately 49% of the most extreme European precipitation events are associated with a COL. Furthermore, we find that the statistical significance of trends in the annual number of COLs associated with precipitation extremes depends on both the precipitation threshold used to define extremes and the season considered.

In a second step, the same detection algorithm is applied to Z500 fields from six Earth System Models (ESMs) participating in the CMIP6 experiments recommended for EURO-CORDEX downscaling. We show that these state-of-the-art ESMs exhibit a negative bias in the simulated number of COLs over the historical period (1981–2014), which is particularly pronounced over the Mediterranean basin. Using bias-adjusted precipitation fields, precipitation events in each ESM are then attributed to COLs under the SSP5-8.5 scenario. As in the reanalysis, trends in the number of COL-associated events depend on the precipitation threshold.

Overall, this study provides new insights into the past and future synoptic-scale impacts of COLs over Europe and supports the interpretation that observed trends in extreme precipitation are primarily thermodynamically driven rather than dynamically. Because the proposed algorithm relies solely on Z500 fields—an accessible and widely available dataset—it can be readily applied to other reanalysis products or climate model outputs, offering a practical tool for assessing model performance in representing COL occurrence over specific regions.

Keywords. Cut-off low, Extreme precipitation, Europe

https://doi.org/10.5194/egusphere-2026-2315
Preprint. Discussion started: 20 May 2026

1 Introduction

In recent years, cut-off lows (COLs) have been responsible for several major flooding events across Europe. In September 2024, Central Europe was affected by Storm Boris (ECMWF, 2024), which triggered widespread flooding. This was followed by the devastating floods in Valencia in October 2024 (Rodero Astaburuaga, 2025). Meanwhile, parts of Belgium and Germany are still recovering from the catastrophic floods of July 2021 (Kreienkamp et al., 2021; Dewals et al., 2021). A COL is a cold-core upper-level depression that becomes isolated from the main westerly flow as a result of large-amplitude jet stream meanders (Eumetsat, 2024). The cold-core nature of these systems is associated with strong horizontal temperature gradients and enhanced vertical instability, both of which can substantially increase precipitation potential. Understanding how the frequency and impacts of COLs may evolve under future climate conditions is therefore an important research question.

Research on the future evolution of COLs remains relatively limited, with only a few studies having explicitly addressed potential changes in their occurrence. For example, Mishra et al. (2025) showed that the frequency of particularly long-lasting COLs could increase in the future, based on analyses of both historical reanalyses and Earth System Model (ESM) projections. They further suggested that, under climate change, the typical COL season may extend into spring. By identifying circulation analogues to the July 2021 event, Thompson et al. (2024) similarly found that longer-lasting COLs may become more frequent in the future. However, their results also indicate that analogue-based approaches may be ill-suited for detecting COLs, as these systems often exhibit highly variable spatial structures.

Using NCEP (National Centers for Environmental Prediction) reanalysis data, Muñoz et al. (2020) reported positive significant trends in the annual number of COLs over the Northern Hemisphere and Europe, based on a detection algorithm relying on isolated low-pressure systems associated with eastward-propagating thermal fronts. For a more comprehensive overview of previous efforts to detect and characterize COLs, the reader is referred to the review provided by Muñoz et al. (2020).

In parallel, Barnes et al. (2023) examined slow-moving cyclones over Australia and found that approximately 72% of extreme precipitation events were associated with such systems. Focusing on southern Europe, Ferreira (2021) used a pseudo–global warming framework under a high-emissions scenario and showed that precipitation intensities associated with COLs could increase by up to 88% over Spain, identifying the Valencia region as a potential hotspot several years before the observed flooding.

In this paper, we present an objective algorithm based on image analysis techniques that enables the systematic attribution of precipitation events to COLs. The primary objective is to attribute high-impact precipitation events over Europe, identified using ERA5 reanalysis data for the period 1940–2024, to dynamically detected COLs. In contrast to previous approaches that either focus solely on circulation patterns or directly analyse precipitation extremes, our framework explicitly separates the dynamical occurrence of COLs from their associated precipitation impacts. This allows us to disentangle changes in COL frequency from changes in precipitation intensity.

Moreover, this framework provides the opportunity to construct a consistent climatology of COL occurrence over Europe during the historical period. As a second application, the same methodology is applied to outputs from six ESMs, using bias-adjusted daily precipitation fields regridded to the ERA5 grid over a historical period (1981–2014) and a future period under

https://doi.org/10.5194/egusphere-2026-2315
Preprint. Discussion started: 20 May 2026

the SSP5-8.5 scenario. The selected models belong to the subset of ESMs recommended for EURO-CORDEX downscaling experiments (Sobolowski et al., 2025). Brajkovic et al. (2025) and Kendon et al. (2023) recently showed that, for rare extreme precipitation events, analyses based on Climate Model outputs suggest that natural variability may play a dominant role in determining the timing of the most extreme occurrences. The present study therefore provides an opportunity to investigate the role of natural variability in the occurrence and impacts of COLs during the historical period and in future simulations, using a consistent attribution framework.

This article is structured as follows. Section 2 describes the detection algorithm and the datasets used in the study. In section 3, we first analyse the evolution of COL occurrence in the ERA5 reanalysis, followed by an attribution analysis using selected CMIP6 model simulations. For each results subsection, a trend analysis is performed to identify statistically significant changes in the annual number of COLs. In addition, regions most affected by COL-related precipitation are identified, allowing the characterization of precipitation hotspots. Finally, Section 4 discusses the limitations of the methodology and highlights potential extensions and applications for future research.

2 Methods and Materials

2.1 COL detection algorithm

The detection of COLs relies exclusively on the dynamical characteristics of isolated low-pressure systems in the 500 hPa geopotential height (z_{500}) field. While previous studies have used either potential vorticity (PV) anomalies (Barnes et al., 2023) or temperature gradients to detect thermal fronts (Muñoz et al., 2020), we focus on z_{500} as it provides a dynamically consistent and temporally homogeneous variable in the ERA5 reanalysis. In addition, mid-tropospheric geopotential height fields are generally less sensitive to changes in data assimilation practices than surface or hydrometeorological variables (Hersbach et al., 2020). COLs typically originate in polar or subpolar regions and become detached from the main westerly flow due to large-amplitude jet stream meanders, appearing as closed depressions in the mid-tropospheric circulation (Fig. 1a; (Muñoz et al., 2020)). In the z_{500} field, such systems are characterized by closed isohypses forming isolated minima.

Detection of closed geopotential structures

For each synoptic configuration, a histogram of z_{500} values is constructed over the analysis domain (Fig. 1b). A cubic spline is fitted to this distribution in order to identify local extrema, which are then used to define two threshold values delimiting the range of geopotential heights within which closed contours are most likely to occur. Specifically, the lower threshold corresponds to the first local minimum, and the upper threshold to the second local maximum of the fitted curve (Fig. 1b). This approach enables the identification of isolated mid-tropospheric low-pressure systems embedded between the climatologically lower geopotential heights at higher latitudes and the higher geopotential values typically found further south. In other words, it filters out the dominant large-scale background circulation.

https://doi.org/10.5194/egusphere-2026-2315
Preprint. Discussion started: 20 May 2026

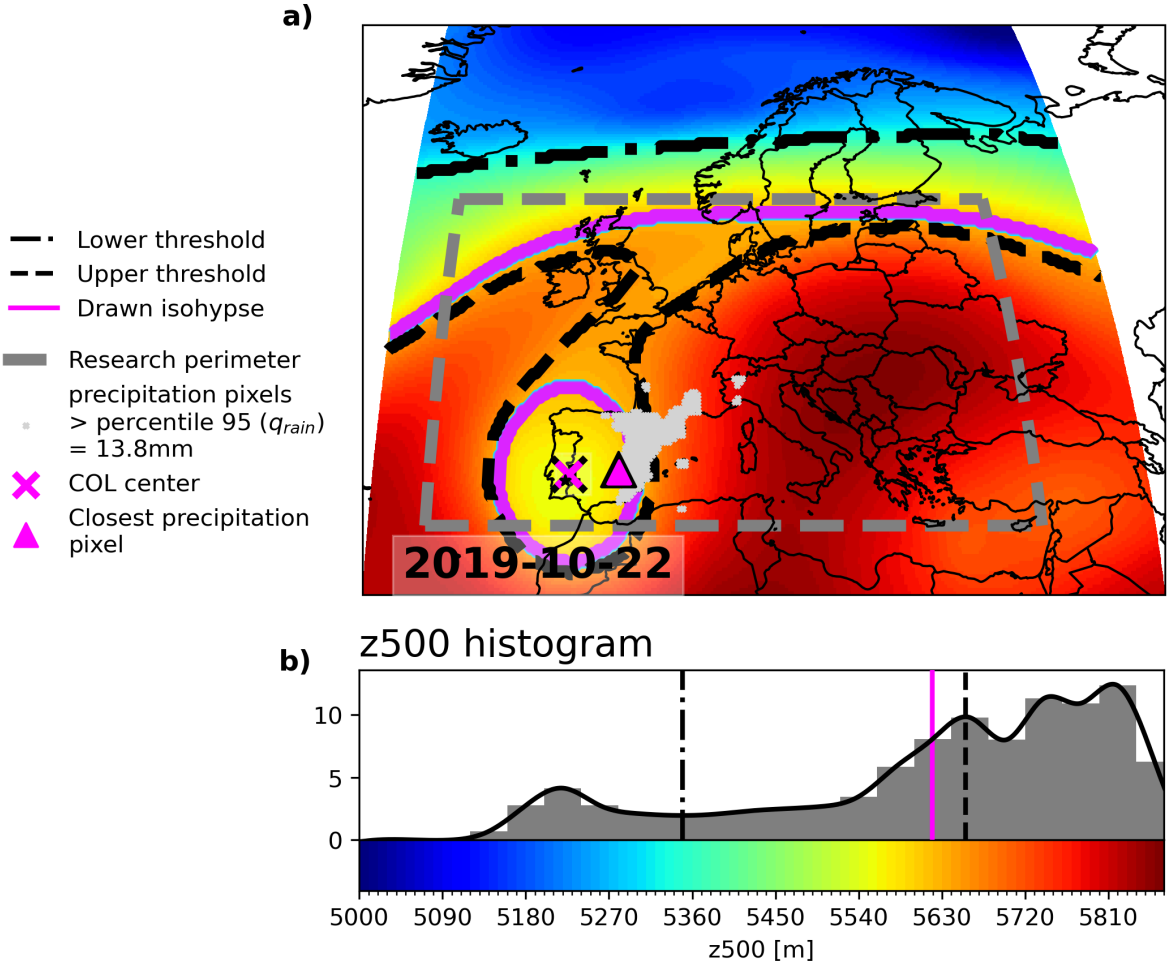

Figure 1. Illustration of the cut-off low (COL) detection algorithm. (a) Example of a closed geopotential structure detected in the 500 hPa geopotential height (z_{500}) field on 22 October 2019, with the magenta contour outlining the closed isohypses and the cross marking the COL center. (b) Histogram of z_{500} values showing the dynamically derived lower and upper thresholds used to guide the identification of closed contours.

Isohypses are subsequently drawn at 10 m intervals within this range. The procedure continues iteratively until at least one closed contour is identified. Each closed contour is then evaluated against the following dynamical and geometrical criteria to determine whether it qualifies as a COL:

1. The area enclosed by the closed contour must exceed a critical threshold of $A_{\text{crit}} = 50{,}000$ km^2. This value is chosen to exclude small-scale, short-lived geopotential anomalies that are not representative of mature synoptic-scale COLs, such as transient upper-level troughs embedded in the large-scale flow. The sensitivity of the results to the definition of A_{crit} is further discussed in Section 4.1.

https://doi.org/10.5194/egusphere-2026-2315
Preprint. Discussion started: 20 May 2026

2. The center of the enclosed area must lie within a predefined domain, bounded by latitude (φ) and longitude (λ):

$$\varphi_{\min} < \varphi < \varphi_{\max}, \quad \lambda_{\min} < \lambda < \lambda_{\max}.$$

At this stage, it is important to note that the detection of COLs relies solely on the structure of the z_{500} field. No precipitation-related information is used to identify closed geopotential systems. Because the analysis is based on daily averaged z_{500} fields, only systems that persist at least over the daily time scale are detected, thereby excluding short-lived transient features.

To improve robustness, the detection algorithm is applied using multiple histogram class widths ranging from 20 m to 110 m in steps of 10 m. For each iteration, the thresholds are recalculated and the search for closed contours is repeated. This multi-resolution approach ensures that the detection is not sensitive to a specific binning choice and allows the algorithm to adapt to varying synoptic configurations.

Attribution of precipitation to detected COLs

Once a COL has been dynamically detected, precipitation is attributed in a second step. A detected COL is classified as precipitation-associated if at least one precipitation grid cell located within the closed geopotential domain exceeds the daily spatial 95th percentile of precipitation ($q_{rain} = 95$) (Fig. 1a), computed over the analysis domain for the same day. This relative, day-dependent threshold accounts for spatial variability in precipitation intensity and avoids excluding dynamically relevant COLs whose precipitation maxima may be spatially displaced.

Importantly, this precipitation criterion does not influence the detection of closed geopotential structures and is used solely to distinguish between dry COLs and COLs associated with potentially impactful precipitation. The sensitivity of the results to the choice of the spatial precipitation quantile is further discussed in Section 4.1. The detection of COLs is not restricted to the impact domain itself but is instead carried out over a broader research perimeter (purple dashed contour in Fig. 2).

2.2 Studied domain and input data

2.2.1 European domain

The analysis focuses on a single European domain designed to capture the large-scale influence of COLs on extreme precipitation, while excluding high-latitude systems governed by distinct dynamical mechanisms (Tamarin and Kaspi, 2017). The domain extends from approximately 35°N to 60°N in latitude and from 20°W to 35°E in longitude (red contour in Fig. 2). This region encompasses Western, Central, and Southern Europe, including the Mediterranean basin.

The Baltic and northern Scandinavian regions are deliberately excluded, as the present study does not aim to investigate polar depressions or fast-moving baroclinic cyclones, whose dynamics and precipitation processes differ substantially from those of COLs.

ERA5 daily precipitation fields are used to characterize precipitation extremes, while ERA5 500 hPa geopotential height (z_{500}) fields are employed for the dynamical detection of COLs. The ERA5 input data cover the period 1940–2024 (Hersbach et al., 2020).

https://doi.org/10.5194/egusphere-2026-2315
Preprint. Discussion started: 20 May 2026

CMIP6 ESM	Member	TCR (K)	Atm. horiz. res.
MIROC6	r1ip1f1	1.55	∼1.4°×1.4°
NorESM2-MM	r1ip1f1	1.33	∼1.0°×1.0°
MPI-ESM1-2-HR	r1ip1f1	1.66	∼0.9°×0.9°
EC-Earth3-Veg-HR	r1ip1f1	2.62	∼0.7°×0.7°
CMCC-CM2-SR5	r1ip1f1	2.09	∼1.0°×1.0°
IPSL-CM6A-LR	r1ip1f1	2.32	∼2.5°×1.3°

Table 1. ESMs used to force MAR at its lateral boundaries (modified after Sobolowski et al. (2025)). TCR = Transient Climate Response.

2.2.2 Input data

For the historical period (1940–2024), the ERA5 reanalysis is used, with a horizontal resolution of 0.25° × 0.25° (Hersbach et al., 2020). The z_{500} fields correspond to daily means, while precipitation fields are daily accumulations.

For climate projections, six ESMs are analyzed under both historical (1981–2014) and SSP5-8.5 (2015–2100) scenarios. These models belong to the subset recommended for EURO-CORDEX dynamical downscaling experiments (Sobolowski et al., 2025) (Table 1). Since the detection algorithm relies on the spatial extent of COLs, daily z_{500} fields from each ESM are regridded to the ERA5 grid using a distance-weighted average of the four nearest model grid points. This ensures that COL detection is not biased by differences in horizontal resolution among the ESMs.

ESM precipitation fields are bias-adjusted using a quantile-mapping approach, specifically the Equidistant Quantile Mapping (EDCDFm) method (Pierce et al., 2015). Prior to bias adjustment, precipitation fields are regridded to the ERA5 grid. ERA5 precipitation is used as the reference dataset over the 1981–2010 calibration period to correct daily precipitation values at each grid cell. The correction factors are season-dependent and differ between extreme and non-extreme precipitation days. This approach is similar to that employed by Brajkovic et al. (2025) and ensures consistent comparisons between COL-related precipitation in ERA5 and ESM datasets.

The selected ESMs exhibit a wide range of Transient Climate Responses (TCRs), defined as the global mean surface temperature increase at the time of CO_2 doubling under a 1% yr^{-1} CO_2 increase scenario (IPCC, 2023). This diversity in climate sensitivity allows the exploration of a range of model responses. For conciseness, the present analysis focuses on the SSP5-8.5 scenario, while results for SSP1-2.6, SSP2-4.5, and SSP3-7.0 are discussed in Section 4.3.

2.3 Application over Europe and trend identification

Extreme precipitation days are identified using spatial precipitation statistics computed over the European domain. For each day, spatial precipitation quantiles are calculated, and precipitation is subsequently attributed to dynamically detected COLs following the methodology described above. The annual number of COL-associated precipitation events exceeding predefined intensity thresholds is then computed.

https://doi.org/10.5194/egusphere-2026-2315
Preprint. Discussion started: 20 May 2026

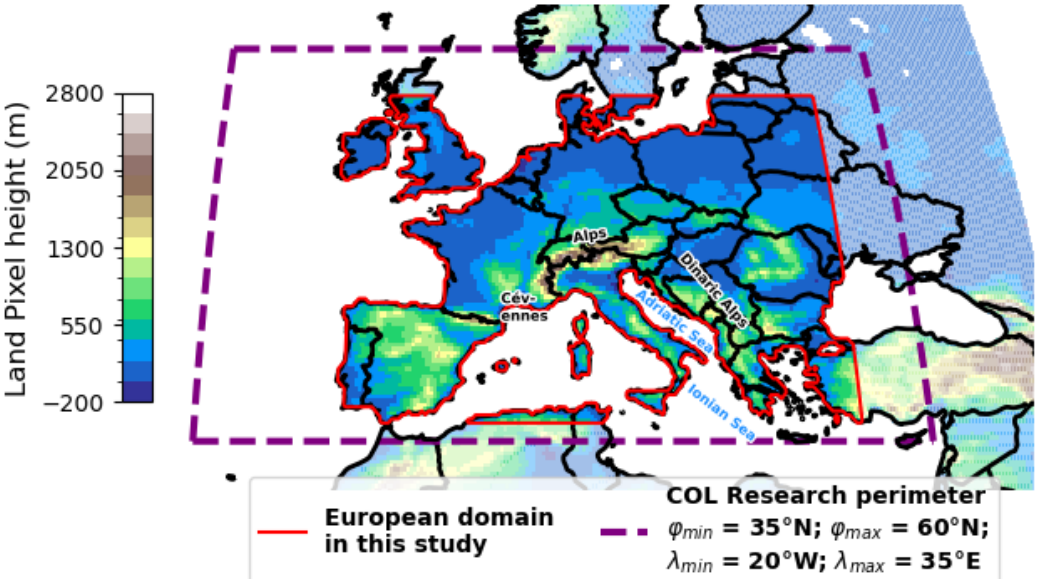

Figure 2. Studied European domain and COL research perimeter. The red contour delineates the European domain used for the analysis of precipitation extremes. The background shading shows ERA5-Land pixel elevations. The dashed purple contour indicates the broader research perimeter within which COLs are dynamically detected ($\varphi_{\min} = 35°\text{N}$, $\varphi_{\max} = 60°\text{N}$, $\lambda_{\min} = 20°\text{W}$, $\lambda_{\max} = 35°\text{E}$). This enlarged perimeter allows the identification of dynamically relevant COLs whose centres may lie outside the precipitation impact domain.

In hydrological and climate sciences, the temporal evolution of counting variables is commonly modeled using a Poisson regression framework (Brajkovic et al., 2025; Tramblay et al., 2013; Grandry et al., 2020). In this context, the probability P_n of observing n COL occurrences in a given year is expressed as:

$$P_n = \frac{\exp(-\gamma)\,\gamma^n}{n!}, \tag{1}$$

where γ denotes the expected annual number of events.

To account for potential temporal trends, γ is modeled as an exponential function of time:

$$\gamma = \exp\left(\gamma_0 + \gamma_1 (y - y_0)\right), \tag{2}$$

where y is the calendar year, y_0 is a reference year corresponding to the beginning of the study period, and γ_0 and γ_1 are regression coefficients estimated from the data. The parameter γ_1 represents the temporal trend in the expected number of COL occurrences.

The statistical significance of the temporal trend is assessed using a Wald test applied to the estimated slope parameter γ_1. A 95% confidence level is adopted throughout the study, such that p-values below 0.05 indicate a statistically significant trend.

https://doi.org/10.5194/egusphere-2026-2315
Preprint. Discussion started: 20 May 2026

A significant result implies that the observed temporal evolution in the number of COLs is unlikely to arise from random variability alone.

3 Results

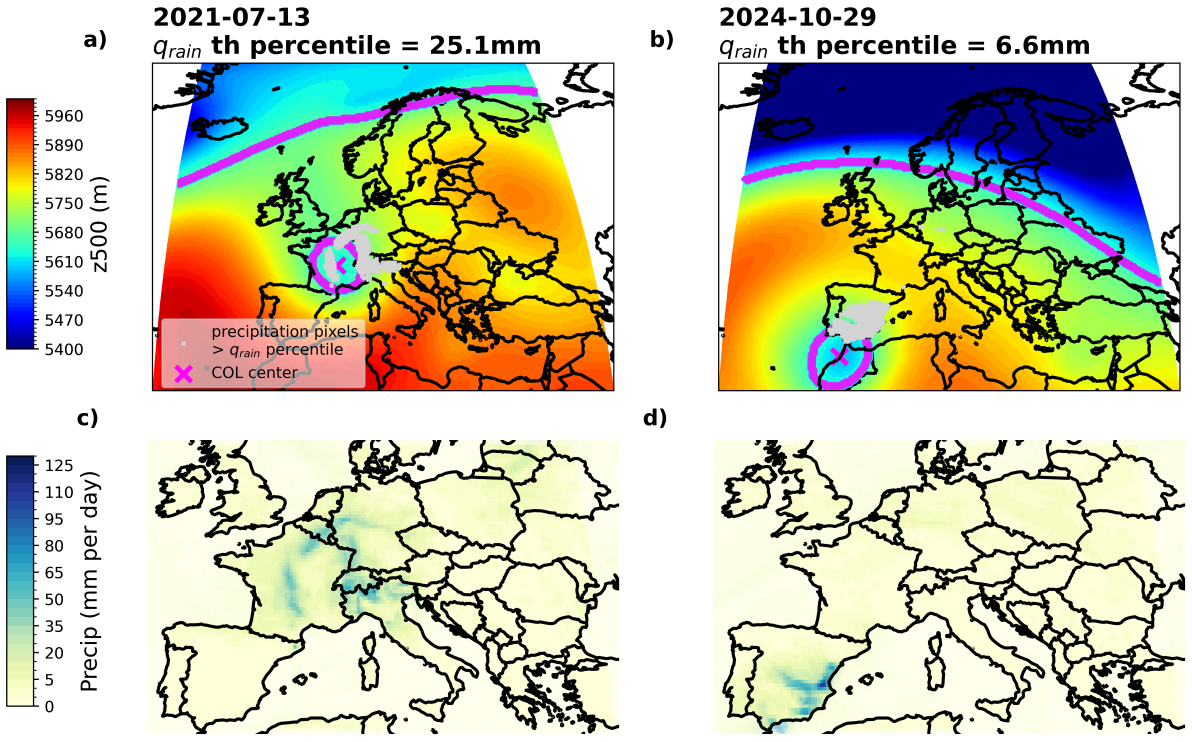

Figure 3. Illustration of the cut-off low (COL) detection and precipitation attribution procedure for two representative events. 500 hPa geopotential height (z_{500}) fields showing dynamically detected closed geopotential structures on 13 July 2021 (a) and 29 October 2024 (b). The magenta contours delineate the closed isohypses identified by the detection algorithm, and the magenta cross marks the corresponding COL center. (c and d) Daily precipitation fields for the same dates.

The applied detection approach allows the systematic attribution of large-scale precipitation events to upper-level COLs in the ERA5 reanalysis. Over the period considered, numerous high-impact precipitation events across Europe are associated with COLs detected by the algorithm (Fig. 3). Depending on their location and structure, COLs can affect a wide range of European regions.

https://doi.org/10.5194/egusphere-2026-2315
Preprint. Discussion started: 20 May 2026

Two recent extreme events illustrate the ability of the algorithm to identify COL-related precipitation impacts. The storm Dana event of October 2024 is clearly detected, with a well-defined upper-level closed low centered near the Gibraltar Strait on 29 October (Fig. 3b). This circulation pattern induced a predominantly south-to-north moisture transport affecting eastern Spain, where daily precipitation totals in ERA5 reached locally up to 120 mm day^{-1} near Valencia (Fig. 3d).

Similarly, the July 2021 event that caused severe flooding in Belgium and eastern Germany is associated with a persistent COL detected by the algorithm (Fig. 3a). In this case, the circulation also exhibits a predominantly meridional flow, although the source region of the moist air masses differs from the Valencia event. While the October 2024 event involved moisture advection from the western Mediterranean, the July 2021 event was associated with air masses originating from Central and Eastern Europe.

3.1 Historical COL impacts

While several recent flooding events were associated with exceptionally intense COL-related precipitation, not all COLs generate extreme rainfall. In the following, we therefore distinguish between the occurrence of COLs irrespective of their precipitation impacts and the subset of COLs associated with extreme precipitation events.

First, we analyse the long-term evolution and spatial distribution of COL occurrence over the studied European domain, independently of precipitation. Second, we attribute historical daily precipitation extremes—defined using high spatial precipitation quantiles—to dynamically detected COLs in order to quantify their contribution to extreme precipitation events.

3.1.1 Evolution of the number of COLs

Periods of enhanced COL activity are noticed in the historical record (Fig. 4a). In particular, the 1970s stand out as a phase of elevated activity, with annual counts exceeding 400 detected COLs in the daily geopotential height fields. This period is preceded and followed by alternating phases of higher and lower COL occurrence, with annual values generally fluctuating around approximately 360 COLs per year. Although these annual counts may appear high relative to the number of days in a year, COLs are counted on a daily basis. Persistent systems are therefore recorded once per day, and multiple COLs may simultaneously occur within the domain.

At the European scale, detected COLs exhibit a non-uniform spatial distribution, with a tendency to cluster around a limited number of preferred regions (Fig. 4b). The spatial counting of COL centres on a regular grid reveals three main activity maxima: (i) south-east of Portugal, (ii) central Italy east of Corsica, and (iii) the Black Sea region. In each of these areas, more than 200 COL centres are detected over the period 1940–2025, whereas regions of lowest activity typically record fewer than 70 events over the same period.

From a seasonal perspective, the highest COL activity is observed in spring (MAM; Fig. 4d), summer (JJA; Fig. 4e), and autumn (SON; Fig. 4f). These three seasons exhibit pronounced inter-decadal variability, with the 1970s clearly standing out as a period of enhanced COL occurrence in all cases. While significant positive tendencies are apparent in JJA and SON, no statistically significant trend is detected for MAM.

https://doi.org/10.5194/egusphere-2026-2315
Preprint. Discussion started: 20 May 2026

In contrast, winter (DJF; Fig. 4c), despite being the least active season in terms of absolute COL counts, exhibits a slight decreasing trend over the study period. The combination of these seasonal evolutions results in the annual COL occurrence (Fig. 4a), which is dominated by inter-decadal variability and shows no significant long-term trend.

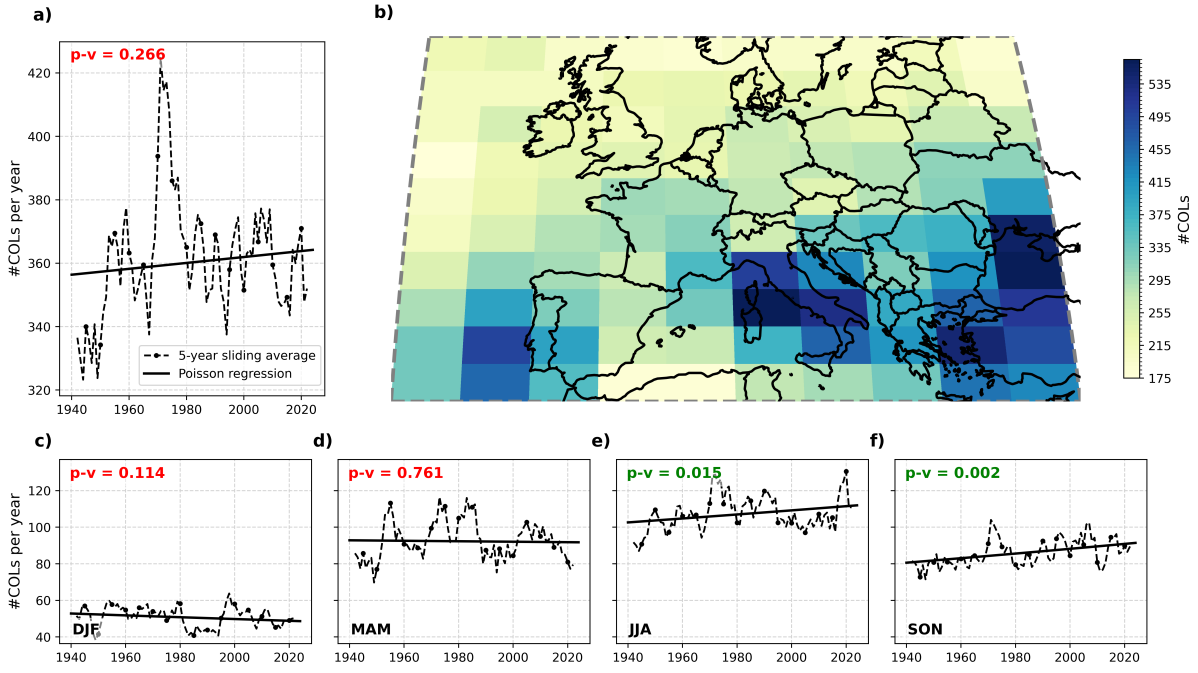

Figure 4. Evolution of cut-off low (COL) occurrence over Europe in ERA5. (a) Annual number of detected COLs over the European domain for the period 1940–2025. The dashed line shows the 5-year running mean and the solid line indicates the Poisson regression fit; the associated p-value is reported (green: statistically significant at the 95% confidence level; red: non-significant). (b) Spatial distribution of COL centres, expressed as the cumulative number of detected COLs over the same period. (c–f) Seasonal evolution of the annual number of COLs for winter (DJF), spring (MAM), summer (JJA), and autumn (SON). Dashed lines represent 5-year running means, solid lines correspond to Poisson regression fits, and reported p-values indicate the statistical significance of the temporal trends. For a more detailed figure with spatial counts per season, see Appendix Figure A1. An algorithm sensitivity test for the A_{crit} parameter is presented in Appendix Figure A2.

3.1.2 Attribution of historical precipitation events to COLs

Across the European domain, we quantify the fraction of extreme precipitation events associated with COLs. Two precipitation intensity thresholds are considered in the analysis: a lower threshold of 5 mm day^{-1} and a higher threshold of 50 mm day^{-1}. These thresholds are selected to distinguish between a broad set of precipitation events potentially influenced by COLs and a subset of high-impact, intense events. For each day, events are identified when the spatial 99.9th percentile of daily precipitation over the European domain exceeds the selected threshold, after which they are attributed to dynamically detected COLs (Fig. 5).

https://doi.org/10.5194/egusphere-2026-2315
Preprint. Discussion started: 20 May 2026

It is important to note that this percentile-based event definition differs from the q_{rain} parameter used in the attribution step. The 99.9th percentile is computed to determine whether a given day qualifies as an extreme precipitation event at the domain scale, whereas q_{rain} is used to identify the precipitation grid cells within the detected COL area for that specific day.

The analysis is performed for the whole year (Y) as well as for the MAM, JJA, and SON seasons. Winter is excluded for conciseness and because it is the season least affected by COL activity.

On an annual basis, approximately 49% of extreme precipitation events are attributed to COLs when using the 5 mm day^{-1} threshold (Fig. 5a). The corresponding time series exhibits pronounced interannual and decadal variability, with periods of enhanced COL-related activity during the 1950s, 1970s, and 2000s, reaching up to about 200 COL-attributed events per year. Despite this variability, no statistically significant long-term trend is detected for this lower threshold, with annual values fluctuating around approximately 180 events per year.

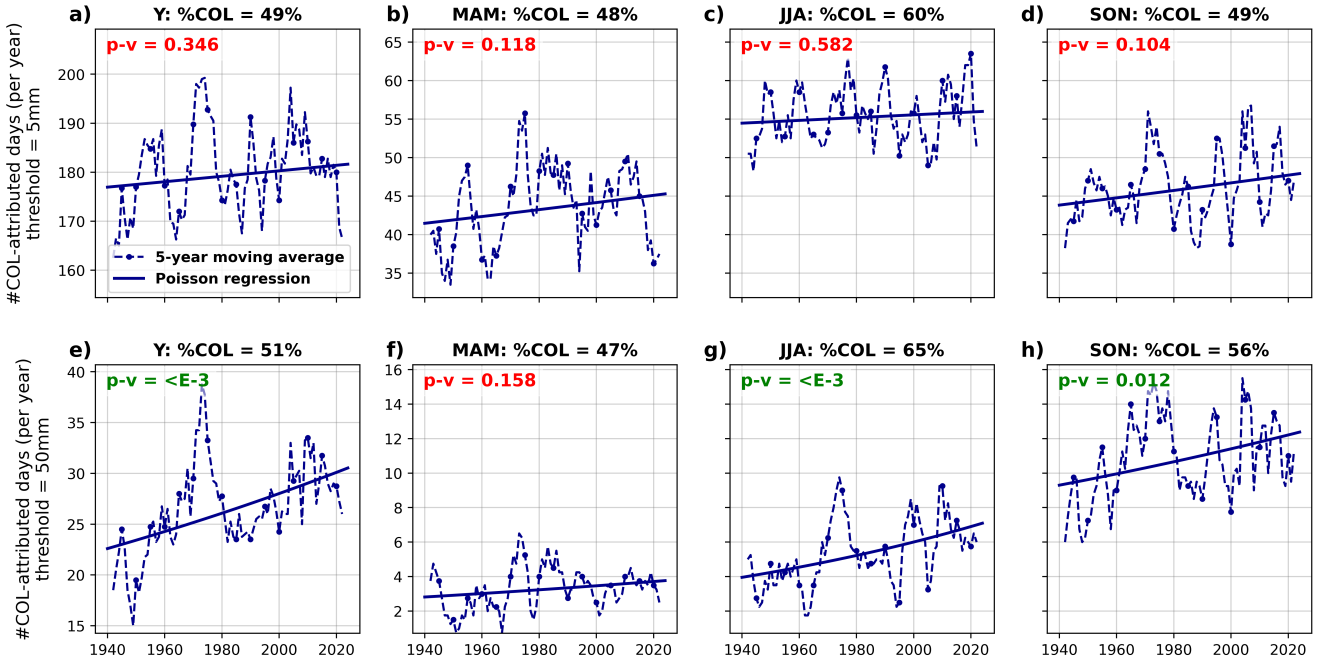

Figure 5. Annual and seasonal evolution of the number of extreme precipitation days attributed to cut-off lows (COLs) in ERA5. Panels (a–d) show the number of days per year exceeding the spatial 99.9th percentile of daily precipitation and reaching at least 5 mm day^{-1}, attributed to COLs, for the whole year (a), MAM (b), JJA (c), and SON (d). Panels (e–h) show the same diagnostics using a stricter precipitation threshold of 50 mm day^{-1}. Dashed lines represent 5-year running means, while solid lines correspond to Poisson regression fits. Reported p-values indicate the statistical significance of the temporal trends (green: statistically significant at the 95% confidence level; red: non-significant).

In contrast, applying the higher threshold of 50 mm day^{-1} yields a markedly different behaviour. In this case, the temporal evolution shows a statistically significant positive trend (Fig. 5e). The 1970s again emerge as a period of elevated COL activity, with up to 40 COL-attributed events per year exceeding the threshold. Over the full 1940–2024 period, the Poisson regression

https://doi.org/10.5194/egusphere-2026-2315
Preprint. Discussion started: 20 May 2026

indicates an increase in the expected annual number of COL-induced extreme events from approximately 24 to 30. This suggests that while moderate COL-related precipitation events exhibit no clear long-term trend, the most intense COL-associated precipitation events have become more frequent over time.

From a seasonal perspective, summer (JJA) emerges as the season most affected by COL activity, with 60% and 65% of events attributed to COLs for the lower and higher thresholds, respectively (5c and g). Using the lower threshold of 5 mm day^{-1}, no statistically significant trend is detected, with annual counts remaining close to 55 COL-attributed events per year (Fig. 5c).

When applying the higher threshold of 50 mm day^{-1}, a statistically significant positive trend is identified. In this case, the expected annual number of COL-induced extreme precipitation events rises to approximately 7 events per year in recent decades (Fig. 5g). With this higher threshold, more events are actually found in SON, which also shows a statistically significant positive trend, rising to approximately 12 events per year in recent decades.

For MAM, the number of COL-attributed events exhibits a positive tendency for both thresholds, although this increase does not reach statistical significance. In autumn (SON), a positive tendency is also apparent, but only for the higher precipitation threshold.

3.1.3 Historical COL impact locations

COLs have long contributed to extreme precipitation events across Europe. To identify the regions most frequently affected, we mapped the number of days on which COL-associated precipitation exceeded 15 mm day^{-1}. This threshold was selected to ensure that at least one COL-related precipitation event affected each grid cell within the European domain.

The region most frequently impacted by COL-related precipitation is located in the southern Dinaric Alps, in the vicinity of Montenegro (Fig. 6a). Over the period 1940–2023, this area experienced approximately 500 COL-attributed precipitation days. Additional regions with similarly high frequencies are found in parts of the European Alps.

These regions are characterized by pronounced topographic gradients (Fig. 2), which favour orographic uplift. In coastal mountain ranges such as the Dinaric Alps, moist maritime air masses from the Adriatic Sea as well as continental air masses can be forced upslope, enhancing precipitation during COL events. A similar enhancement is observed over the mountainous regions of western Greece bordering the Ionian Sea.

The influence of topography is further evident when examining the mean precipitation associated with COLs (Fig. 6b). The southern Dinaric Alps again emerge as a major hotspot, exhibiting both high frequencies and high intensities of COL-related precipitation. Other prominent topographic features are also visible, including the Apennines, the Cévennes Massif, and the Iberian mountain ranges. These areas consistently coincide with enhanced COL-induced precipitation.

However, elevated COL-related precipitation is not restricted to mountainous regions. Flatter areas such as eastern Germany also exhibit relatively high impacts, indicating that topography alone does not fully explain the spatial distribution of COL-associated precipitation.

The spatial patterns of COL-induced precipitation are broadly consistent with the preferred locations of COL centres identified independently of precipitation intensity (Fig. 4b). In particular, the three main regions of enhanced COL occurrence—south-

https://doi.org/10.5194/egusphere-2026-2315
Preprint. Discussion started: 20 May 2026

east of Portugal, central Italy, and the Black Sea region—help explain why southern European mountain ranges, including the Iberian Peninsula, the southern Alps, and the Balkans, concentrate a large fraction of high-impact COL events.

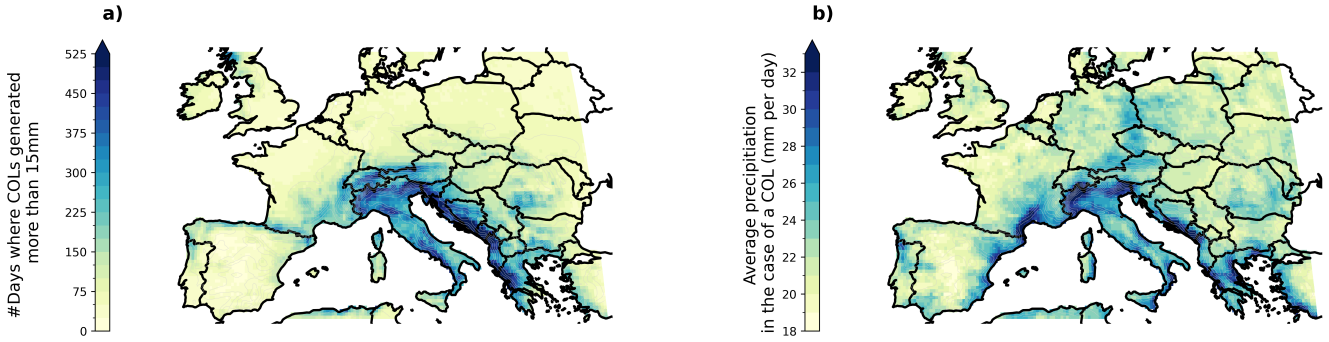

Figure 6. Spatial distribution of cut-off-low (COL)–associated precipitation impacts over Europe for the period 1940–2024. (a) Number of days on which COL-associated precipitation exceeds 15 mm day^{-1}. (b) Mean daily precipitation amount associated with COLs (mm day^{-1}). Both panels highlight regions frequently affected by COL-driven precipitation as well as areas where COLs produce higher average rainfall intensities.

3.2 Evolution of COL impacts in Earth System Models

The historical evolution of COL-induced precipitation events exhibits pronounced natural variability. In this section, we first assess how well the selected ESMs reproduce the frequency and spatial distribution of COLs over the historical period. We then examine the projected evolution of COL-related precipitation impacts as simulated by these models.

3.2.1 Historical representation of COL occurrence by ESMs

The selected ESMs exhibit varying skill in representing COL occurrence independently of any precipitation attribution. When analysing the evolution of the total number of detected COLs over the historical period, a pronounced inter-decadal variability is evident in all models, similar to that observed in ERA5 (Fig. 7a).

However, the absolute number of simulated COLs is systematically underestimated by the ESMs compared to ERA5. MIROC6 and EC-Earth3-Veg provide the closest agreement with ERA5, with annual counts fluctuating around 300 COLs per year (Fig. 7a). In contrast, CMCC-CM2-SR5 and NorESM2-MM exhibit the strongest underestimation, with approximately 210 identified COLs per year. Finally, MPI-ESM1-2-HR and IPSL-CM6A-LR fall between these two groups, with annual counts around 250 COLs per year.

This overall underestimation is also reflected in the spatial distribution of COL occurrence. All ESMs exhibit their largest negative biases over the Mediterranean basin, a feature that is particularly pronounced in NorESM2-MM and CMCC-CM2-SR5 (Fig. 7e and f). As a result, the three main regions of enhanced COL activity identified in ERA5 are not reproduced by the models.

https://doi.org/10.5194/egusphere-2026-2315
Preprint. Discussion started: 20 May 2026

The spatial anomaly patterns (Figs. 7b–g) indicate that COL occurrence is preferentially shifted northwestward in the ESMs compared to ERA5 (Fig. 4b). For example, MIROC6—despite providing the closest agreement with ERA5 in terms of total COL counts—shows a positive bias over the North Atlantic while underestimating COL activity over the Mediterranean basin and the Black Sea region.

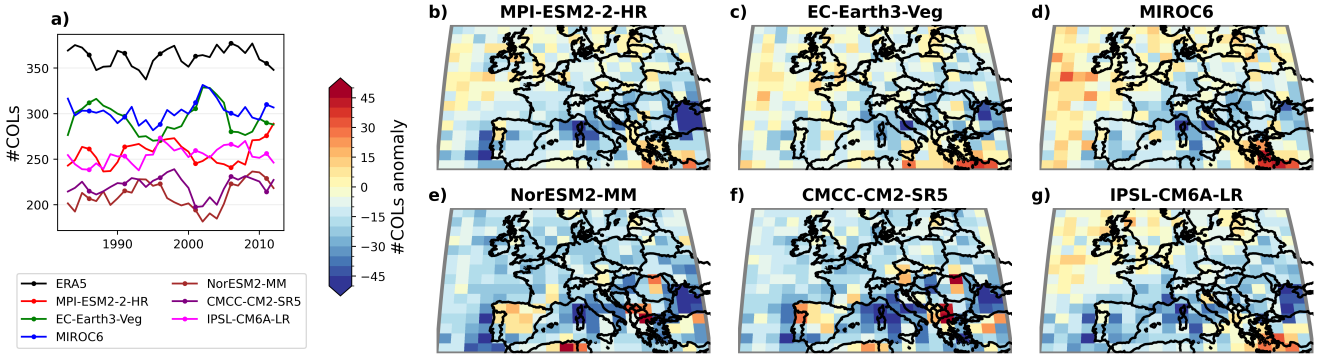

Figure 7. Evaluation of cut-off low (COL) occurrence in CMIP6 ESMs relative to ERA5 over the historical period (1981–2014). (a) Annual number of detected COLs in ERA5 and in the selected ESMs (see Table 1), with a 20-year running mean applied. (b–g) Spatial anomalies in the cumulative number of detected COL centres in each ESM relative to ERA5 over the same period.

3.2.2 Attribution of projected extreme precipitation events by ESMs

Using the same attribution methodology as for ERA5 (Section 3.1.2), future extreme precipitation events simulated by the ESMs under the SSP5-8.5 scenario are attributed to potential COLs. When applying the lower 5 mm day^{-1} threshold, all ESMs exhibit a decrease in the annual number of COL-associated precipitation events, in contrast to the absence of a significant trend in ERA5 over the historical period (Fig. 8a).

In addition to these differing trends, the absolute number of COL-related events is systematically underestimated by the models. Two distinct groups emerge: one characterized by stronger underestimation (NorESM2-MM, CMCC-CM2-SR5, and IPSL-CM6A-LR) and another showing closer agreement with historical ERA5 counts (EC-Earth3-Veg, MIROC6, and MPI-ESM1-2-HR). This grouping remains consistent across precipitation seasons regarding this lower threshold (Fig. 8).

When the higher threshold of 50 mm day^{-1} is applied, a behaviour similar to that observed in ERA5 emerges for three models, namely MIROC6, NorESM2-MM and EC-Earth3-Veg (Fig. 8e). In these models, COL-associated extreme precipitation events exhibit statistically significant positive trends, although the simulated event counts generally remain below historical ERA5 levels. An exception is EC-Earth3-Veg, which reaches values comparable to those observed in ERA5 by the end of the century.

From a seasonal perspective, spring (MAM) shows the strongest inter-model agreement in future trend behaviour under the higher 50 mm day^{-1} threshold. All ESMs exhibit increasing tendencies in the number of COL-associated extreme precipitation

https://doi.org/10.5194/egusphere-2026-2315
Preprint. Discussion started: 20 May 2026

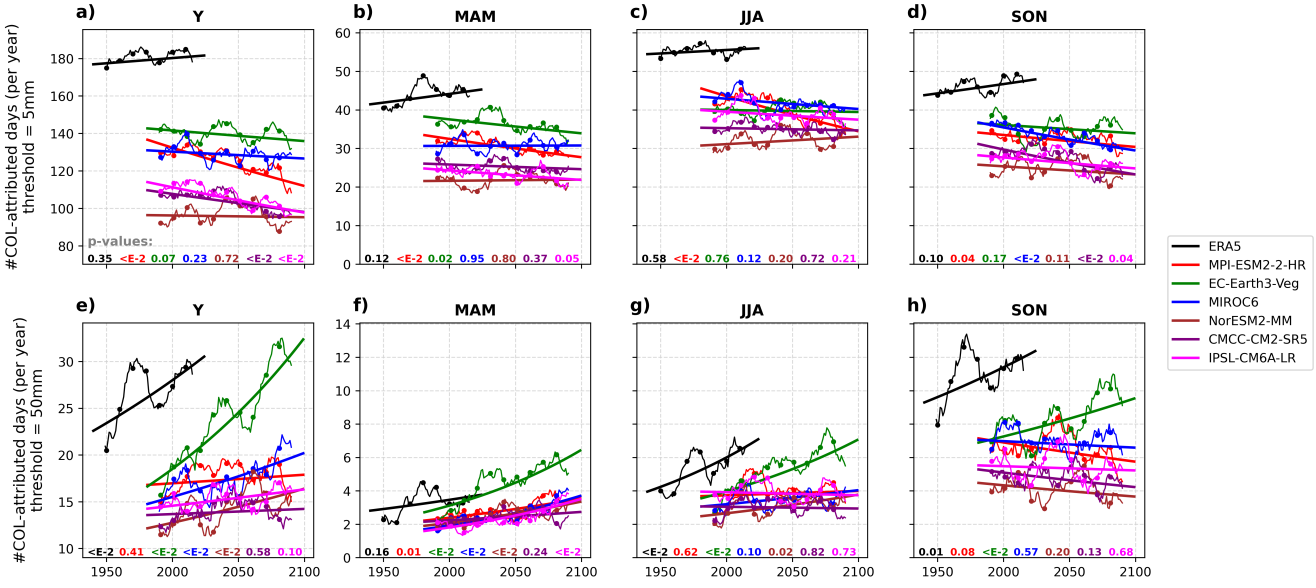

Figure 8. Evolution of the annual and seasonal number of extreme precipitation days attributed to cut-off lows (COLs) in ERA5 and CMIP6 ESMs. Panels (a–d) show the annual number of days exceeding the spatial 99.9th percentile of daily precipitation and reaching at least 5 mm day^{-1}, attributed to COLs, for the whole year (a), MAM (b), JJA (c), and SON (d). Panels (e–h) show the same diagnostics using a stricter precipitation threshold of 50 mm day^{-1}. Black curves correspond to ERA5 over the historical period, while coloured curves show CMIP6 ESM projections under the SSP5-8.5 scenario. Dashed curves represent 20-year running means, while solid lines indicate Poisson regression fits used to assess temporal trends. Associated p-values are displayed at the bottom of each panel in the colour corresponding to the respective curve.

events (Fig. 8f). EC-Earth3-Veg stands out in particular, exceeding historical ERA5 levels by the end of the century, with more than six events per year during some periods.

In contrast, the systematic underestimation of COL-related extreme precipitation by ESMs is particularly pronounced in autumn (SON) (Figs. 8g–h). For this season, simulated event counts under the higher threshold never reach the levels observed in ERA5. EC-Earth3-Veg is the only model exhibiting increasing trends comparable in sign to those derived from ERA5, although with substantially lower absolute magnitudes.

Beyond the long-term trends, each ESM exhibits its own internal variability, reflecting the natural variability also observed in the reanalysis. In summer (JJA), for example, MPI-ESM1-2-HR displays a period of enhanced COL-related activity at the beginning of the simulation, followed by extended phases of lower activity (Fig. 8g). Similar inter-decadal fluctuations are apparent across all seasons and models, highlighting the strong role of internal variability in modulating COL-related precipitation at multi-decadal timescales.

https://doi.org/10.5194/egusphere-2026-2315
Preprint. Discussion started: 20 May 2026

4 Discussion

This study shows that trends in COL–associated precipitation extremes depend strongly on the precipitation threshold used to define extreme events, and that ESMs systematically underestimate both the occurrence and impacts of COLs over Europe. In this section, we first discuss the sensitivity of the results to key parameters of the detection and attribution algorithm. We then briefly review additional physical mechanisms that may contribute to the observed trends in extreme precipitation beyond changes in COL occurrence alone. Finally, we discuss the broader implications of these findings for the interpretation of past trends and future projections of COL-related extreme precipitation.

4.1 Algorithm limits, strengths, and sensitivity analysis

The main results of this study are not significantly influenced by the predefined parameters of the detection algorithm. However, these parameters do affect the total number of systems identified as COLs.

One parameter that influences the total number of detected COLs is A_{crit}, the critical area that an isolated low-pressure system must reach in order to be classified as a COL. In this study, A_{crit} is set to $5 \times 10^4\,\text{km}^2$. This parameter determines how large and spatially isolated a geopotential minimum must be to be detected.

While variations in A_{crit} affect the absolute number of detected COLs, they do not substantially alter the main conclusions of the study. For example, increasing A_{crit} to $10^6\,\text{km}^2$ results in a systematic downward shift in the annual counts shown in Fig. 4, without affecting the temporal behaviour or the detected trends. Additional sensitivity tests are presented in the Appendix (Figs. A1 and A2).

The q_{rain} parameter controls the spatial criterion used to attribute precipitation extremes to detected COLs. In this study, q_{rain} is set to 95, meaning that a precipitation grid cell is attributed to a COL if its daily precipitation exceeds the spatial 95th percentile and if it lies within the area enclosed by the corresponding z_{500} closed contour (see methodological section 2.1 and Fig. 1).

To assess the sensitivity of the attribution to this parameter, an additional sensitivity analysis was performed using varying values of q_{rain} (Fig. 9). This analysis allows us to evaluate whether the attribution of extreme precipitation events to COLs is robust with respect to the chosen percentile threshold.

Using the lower precipitation threshold of 5 mm day^{-1}, Fig. 9 shows that higher values of q_{rain} lead to a lower proportion of extreme precipitation events attributed to COLs. For instance, when using $q_{\text{rain}} = 99.9$, only 23% of the events are attributed to COLs (Fig. 9d).

This stricter attribution criterion results in an overall downward shift in the annual number of COL-attributed events. Only when using $q_{\text{rain}} = 99.9$ does the trend become statistically significant. However, this value was not retained because it excluded several precipitation events for which the synoptic influence of a COL was clearly identified. Such a threshold would therefore be overly restrictive.

Furthermore, the proposed algorithm offers several advantages. First, it does not require the synoptic feature to exhibit a consistent spatial pattern that can be tracked over time, as is the case for analogue-based approaches. As a result, COLs with

https://doi.org/10.5194/egusphere-2026-2315
Preprint. Discussion started: 20 May 2026

very different spatial signatures can still be detected (see Figs. 3 and 6). This makes the method adaptable to a wide range of COL structures, without imposing explicit spatial constraints.

Second, the algorithm relies on input variables that are widely available, including in ESM outputs, which facilitates its application across different datasets and modelling frameworks. Finally, the sensitivity of the results to key algorithm parameters can be straightforwardly assessed, as demonstrated in this study. This allows for transparent robustness checks and strengthens confidence in the main conclusions.

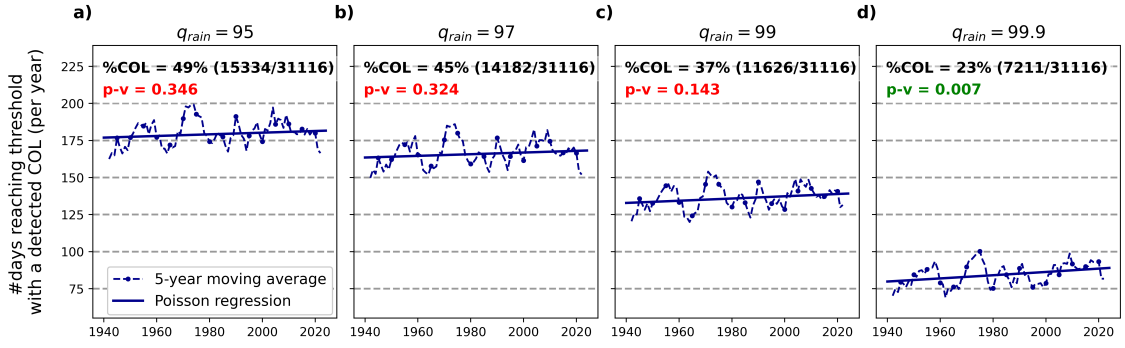

Figure 9. Sensitivity of the attribution of extreme precipitation days to cut-off lows (COLs) with respect to the spatial precipitation quantile used to define COL influence. Panels (a–d) show the annual number of days per year attributed to COLs for spatial precipitation quantiles $q_{\mathrm{rain}} = 95$, 97, 99, and 99.9, respectively. In each panel, dashed curves represent 5-year running means, while solid lines correspond to Poisson regression fits. Percentages indicate the fraction of extreme precipitation days associated with COLs for each quantile, and reported p-values denote the statistical significance of the temporal trends (green: statistically significant at the 95% confidence level; red: non-significant). Additional sensitivity tests, including alternative precipitation thresholds, are presented in Appendix Figures A4–A6.

4.2 Toward a Better Understanding of Physical Drivers Behind COL Impacts

While this study focuses on the detection of COLs and the attribution of extreme precipitation events to these systems, a broader understanding of the physical mechanisms controlling their impacts remains essential. In this section, we discuss several dynamical and thermodynamic drivers that may help interpret the observed results and guide future research.

Recent work by Mishra et al. (2025), based on CMIP6 outputs, suggests that a slowing of mid-latitude atmospheric dynamics under global warming may lead to an eastward shift in the average position of COLs over Europe, as well as an increase in the frequency of particularly long-lasting systems. Their conclusions are derived from projected COL frequency anomalies computed for the 2071–2100 period. Similarly, Muñoz et al. (2020) reported slight long-term trends in COL frequency over Europe for the period 1960–2017. Their analysis relied on NCEP/NCAR reanalysis data and employed a detection method based on isolated low-pressure systems associated with eastern thermal fronts.

In contrast, our analysis highlights the presence of strong inter-decadal variability, including within ESM simulations. Using the detection algorithm developed here, we find no evidence for a systematic long-term increase in the number of detected

https://doi.org/10.5194/egusphere-2026-2315
Preprint. Discussion started: 20 May 2026

COLs on a yearly basis. Instead, the historical record is dominated by pronounced inter-decadal variability, with periods such as the 1970s exhibiting enhanced COL activity and persistence. This period has also been identified in previous studies as a phase of major circulation changes over the North Atlantic–European sector, associated with a climate regime shift (e.g. (Dai et al., 2018; Sarkar and Maity, 2021)).

However, we do find slight but statistically significant positive trends in the JJA and SON seasons (Fig. 4e,f), suggesting that seasonal dynamical changes may influence COL frequency. The significance of these trends is highly sensitive to the inclusion of the 1940–1950 period in the analysis. When restricting the analysis to the same period as Muñoz et al. (2020) (1960–2017), the positive trends disappear and become non-significant (see Fig. A3 for details).

These differences between our results and those of Muñoz et al. (2020) may partly arise from differences in the definition of the European domain, which in their study excludes regions north of the Alps as well as the Azores archipelago. Additionally, differences in input datasets and methodological assumptions—particularly the reliance on frontal structures—may contribute to the discrepancy. In contrast, our approach relies solely on mid-tropospheric geopotential height fields and does not impose thermal or frontal constraints.

Our findings are consistent with recent studies that emphasize the dominant role of thermodynamic processes in shaping future changes in extreme precipitation over Europe. For instance, Pfahl et al. (2017), based on CMIP6 simulations, concluded that projected increases in European precipitation extremes are primarily driven by thermodynamic factors rather than by changes in large-scale circulation patterns. Similar conclusions were reached for Belgium by Schoofs et al. (2025). In line with these results, we show that although the frequency of extreme precipitation events exhibits significant positive trends, this increase is not systematically accompanied by a corresponding rise in COL occurrence. This suggests that past periods of enhanced COL activity exist, but their irregular timing points to a strong contribution from internal climate variability.

Because COLs are frequently associated with the most intense precipitation events in Europe, this internal variability likely contributes to the temporal evolution of extreme precipitation occurrence.

Topography and regional differences in climate change responses may further modulate the observed trends. Moustakis et al. (2020) showed that changes in extreme precipitation intensity across Europe are strongly conditioned by terrain characteristics and local-scale processes. Although our analysis considers Europe as a single domain, marked regional disparities emerge. For instance, extreme precipitation intensity is projected to decrease in parts of the Mediterranean basin, while increasing trends are reported over northern Europe and Scandinavia (Rajczak and Schär, 2017; Coppola et al., 2021). Consistent with these findings, our results confirm that topography plays a key role in amplifying precipitation during COL events, both at continental and local scales.

Despite the absence of a systematic increase in COL frequency, several exceptionally damaging flood events have occurred during the past five years—notably in Belgium, eastern Spain (Valencia), and Central Europe—associated with record-breaking rainfall totals. Many of these events were linked to COLs, suggesting that additional physical mechanisms may have amplified their impacts beyond what would be expected from circulation changes alone. These mechanisms remain insufficiently understood and warrant further investigation.

https://doi.org/10.5194/egusphere-2026-2315
Preprint. Discussion started: 20 May 2026

Recent work by Insua-Costa et al. (2022) demonstrated that approximately 50% of the moisture contributing to the July 2021 extreme precipitation event (daily precipitation on the 13th of July) in eastern Belgium and western Germany originated from local recycling, through evaporation from Central and Northern European forests. Such recycling processes are expected to become more effective under future warming conditions (Fernández-Alvarez et al., 2023), as several regional moisture sources are projected to release larger amounts of water vapour. This highlights the potential importance of land–atmosphere interactions in modulating precipitation intensity during extreme events.

To provide additional context, we briefly examine the evolution of total evapotranspiration across several European regions using ERA5 reanalysis data (Fig. 10). Over recent decades, multiple regions exhibit statistically significant trends in total evapotranspiration during specific months, suggesting that land-surface processes may increasingly influence the atmospheric moisture available for high-impact precipitation events.

In southern Europe, for example, total monthly evapotranspiration shows significant long-term increases in both May and September over the 1940–2023 period. Similarly, key moisture source regions such as the Baltic Sea and the North Sea exhibit significant positive evapotranspiration trends, particularly during April, May, and June (Fig. 10). These changes may contribute to a progressively more humid lower troposphere during the late spring and early summer months.

When combined with enhanced atmospheric instability under warming conditions—such as increased convective available potential energy (CAPE)—these factors could favour more intense convective responses when large-scale dynamical triggers are present (Calvo-Sancho et al., 2026). In this context, Calvo-Sancho et al. (2026) showed that the Dana COL, which struck Valencia in October 2024 (see Fig. 3b and d), produced approximately 20% more heavy precipitation than it would have under pre-industrial conditions, corresponding to an increase of about 55% in the spatial extent of the precipitation event. Their analysis indicates that this intensification is linked to enhanced moisture fluxes from the Mediterranean Sea (about +9%) as well as increased updraft velocities within the associated convective systems.

In this context, COLs may act primarily as synoptic-scale facilitators, while the ultimate severity of extreme precipitation events depends on a complex interplay between atmospheric circulation, land–surface feedbacks, and thermodynamic conditions. These interactions remain insufficiently constrained and represent an important avenue for future research aimed at improving the understanding and prediction of extreme large-scale precipitation events in Europe.

4.3 Implications of the results

Our results highlight the dominant role of natural variability in modulating the annual frequency of COLs over the 1940–2024 period. This strong inter-decadal variability, also reported in recent studies (Brajkovic et al., 2025; Hundhausen et al., 2024; Kendon et al., 2023; Jain et al., 2023), implies that future climate conditions may still be characterized by extended periods of both enhanced and reduced COL activity. Because COLs represent one of the primary synoptic drivers of extreme precipitation in Europe, this variability is expected to translate directly into pronounced fluctuations in the occurrence of extreme precipitation events. However,COLs are expected to become increasingly impactful in the future as the global climate warms. This has already been demonstrated using pseudo-global warming experiments (Thompson et al., 2025; Ludwig et al., 2023) or using model simulations (Ferreira, 2021).

https://doi.org/10.5194/egusphere-2026-2315
Preprint. Discussion started: 20 May 2026

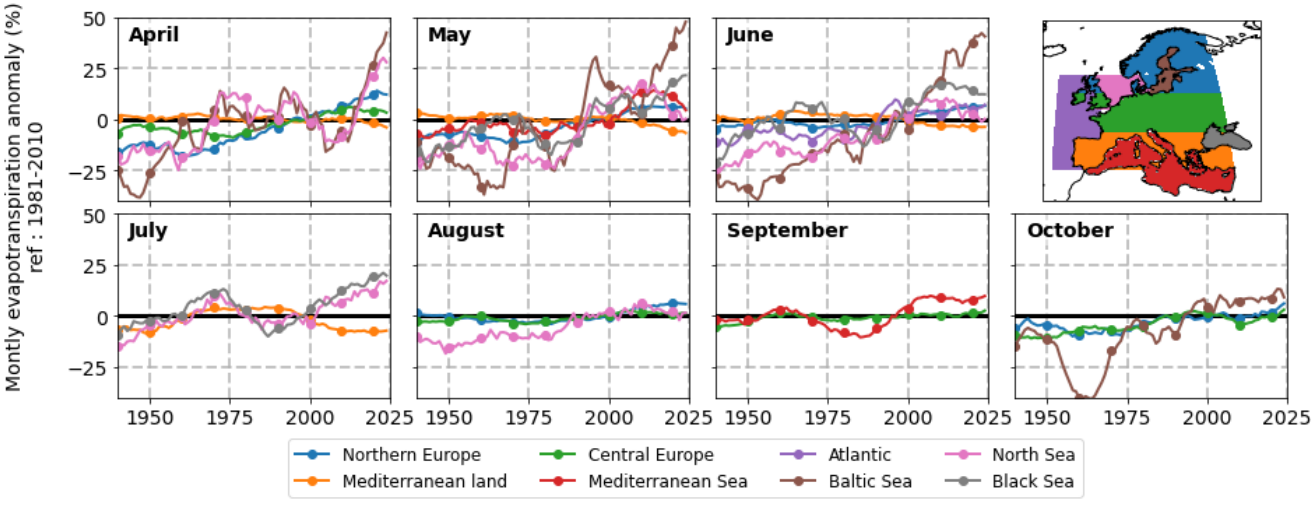

Figure 10. Monthly anomalies of total evapotranspiration (%) over selected European regions based on ERA5 data, expressed relative to the 1981–2010 climatological mean. Linear trends are shown only where they are statistically significant (p-value < 0.05), as determined using a Mann–Kendall test. A 15-year running mean is applied.

This strong natural variability is also reflected in the attribution of future extreme precipitation events simulated by ESMs. All considered ESMs underestimate the occurrence of COLs over Europe, with particularly large biases over Southern Europe. Among the selected models, EC-Earth3-Veg exhibits trends most consistent with those derived from ERA5. Nevertheless, no ESM is able to reproduce the recent observed levels of COL-associated extreme precipitation. In most cases, present-day ERA5 values are only reached—or even exceeded—by the end of the 21st century in EC-Earth3-Veg under the SSP5-8.5 scenario. This finding motivated our focus on this high-emissions scenario, as even under such forcing, simulated COL-related extremes remain lower than those currently observed. Results obtained under the SSP1-2.6 scenario show similar behaviour and are provided in Appendix Figure A7.

Topography emerges as a key modulating factor of precipitation intensity during COL events. Mountainous regions such as the southern Dinaric Alps consistently appear as hotspots of COL-related precipitation impacts. However, COLs are also capable of triggering heavily loaded frontal systems that affect flatter regions, including the Netherlands and Belgium. This indicates that, while some regions are more frequently exposed due to their geographical setting, no part of Europe can be considered immune to the risk of severe COL-associated precipitation.

Finally, these results emphasize the need for further research into the drivers of COL variability and the mechanisms leading to periods of clustered extreme events. In particular, future work should investigate potential low-frequency modes or periodicities in COL occurrence, as well as the combined influence of land–atmosphere feedbacks, moisture availability, and changes in atmospheric stability under climate change. Improving the understanding of these processes is essential for better anticipating the timing and severity of future large-scale precipitation extremes in Europe.

https://doi.org/10.5194/egusphere-2026-2315
Preprint. Discussion started: 20 May 2026

5 Conclusions

In this study, we developed an objective and computationally efficient algorithm based solely on 500 hPa geopotential height fields to detect COLs and to systematically attribute extreme precipitation events to their potential synoptic influence over Europe. Applied to the ERA5 reanalysis over the 1940–2024 period, this approach allowed us to construct a long-term climatology of COL occurrence and to quantify their contribution to extreme precipitation events using a consistent and transparent attribution framework.

Our results show that the total number of COLs over Europe exhibits strong inter-decadal variability but no statistically significant long-term trend. Nevertheless, COLs are found to be associated with a substantial fraction of European precipitation extremes, accounting for approximately half of the most extreme daily events, depending on the precipitation threshold and season considered. Importantly, while moderate COL-related precipitation events show no significant temporal trend, the most intense COL-associated extremes display statistically significant increases, particularly in summer. This threshold dependence highlights that changes in extreme precipitation cannot be inferred from COL frequency alone and points toward a dominant thermodynamic contribution to the observed intensification of extreme events.

When applied to six CMIP6 ESMs, the detection algorithm reveals a systematic underestimation of COL occurrence, especially over the Mediterranean basin, and a northward displacement of simulated COL activity compared to ERA5. Although some models reproduce the sign of observed trends in COL-associated extreme precipitation, none are able to reproduce present-day reanalysis levels, even under the high-emissions SSP5-8.5 scenario. These results suggest that current-generation ESMs struggle to represent both the dynamical characteristics of COLs and their associated precipitation impacts, which has important implications for the interpretation of future projections of extreme precipitation over Europe.

Overall, this study emphasizes that future changes in European extreme precipitation are primarily driven by thermodynamic factors rather than by systematic increases in COL frequency. At the same time, the strong role of natural variability implies that periods of clustered high-impact COL events may continue to occur, even in the absence of clear long-term dynamical trends. The proposed detection and attribution framework provides a flexible and transparent tool that can be readily applied to other regions, reanalysis products, or climate model outputs. Future work should focus on improving the representation of COL dynamics in climate models and on better understanding the interactions between synoptic forcing, land–atmosphere feedbacks, and atmospheric instability that ultimately control the severity of COL-related extreme precipitation events.

Code availability

The cut-off low (COL) detection algorithm developed in this study is publicly available at https://doi.org/10.5281/zenodo.19604862.

The archived version provides the full Python implementation of the method, together with a documented example script and sample datasets enabling reproducibility of the detection workflow.

https://doi.org/10.5194/egusphere-2026-2315
Preprint. Discussion started: 20 May 2026

Data availability

ERA5 reanalysis data are available from the Copernicus Climate Data Store (CDS). CMIP6 data are available via the Earth System Grid Federation (ESGF).

Author contributions

Josip Brajkovic, Sébastien Doutreloup and Nicolas Ghilain conceived the study. Josip Brajkovic developed the algorithm, performed the analysis and led the writing of the manuscript. Nicolas Ghilain and Sébastien Doutreloup contributed to the manuscript structure and writing. Pierre Archambeau provided input on both the methodology and the manuscript.

Appendix

Competing interests. The authors declare that they have no conflict of interest.

Acknowledgements. This study was funded under the BRAIN programme of the Belgian Science Policy Office through the CORDEX.be II research project (contract no. B2/223/P1/CORDEX.be II). AI tools have been used for orthographic and grammar corrections. It was also used as programming assistant for debugging and code optimisation.

https://doi.org/10.5194/egusphere-2026-2315
Preprint. Discussion started: 20 May 2026

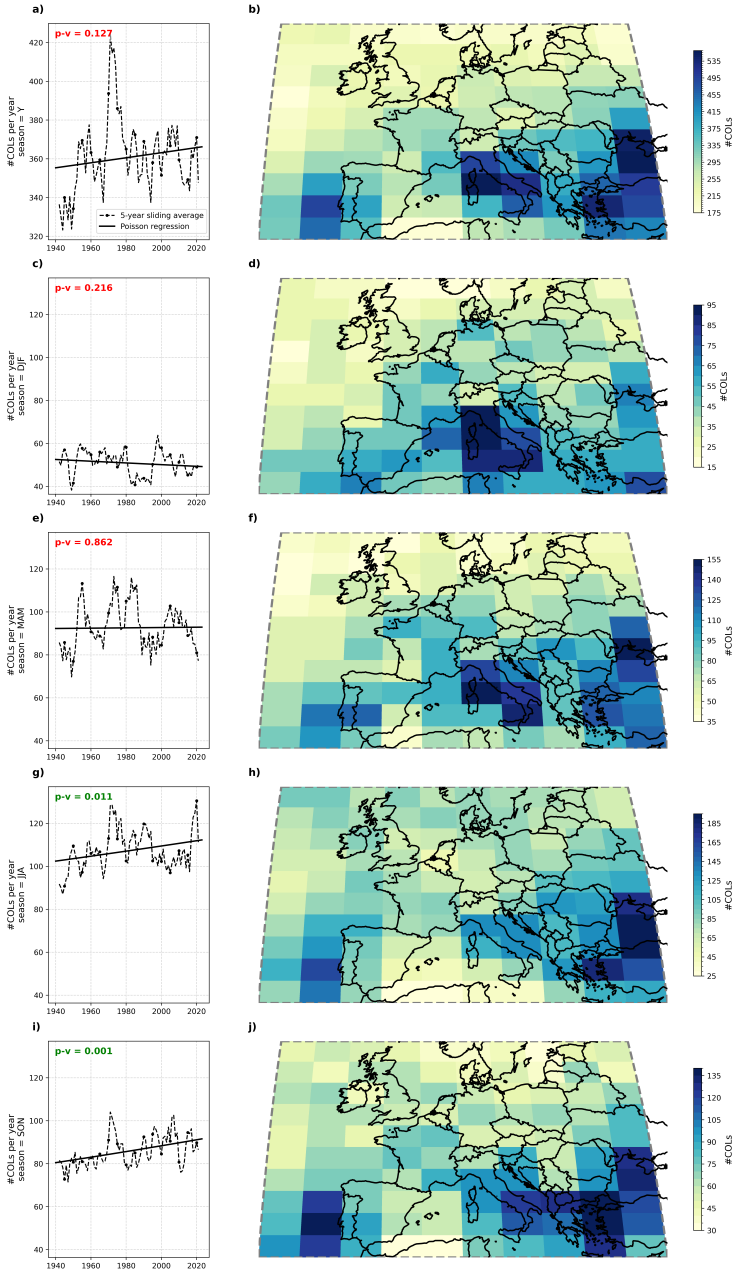

Figure A1. This figure is associated with Figure 4 of the original paper. (a) Annual count of COLs per year and (b) spatially cumulated count over the same period. (c–j) Same as (a–b) but for the other seasons.

https://doi.org/10.5194/egusphere-2026-2315
Preprint. Discussion started: 20 May 2026

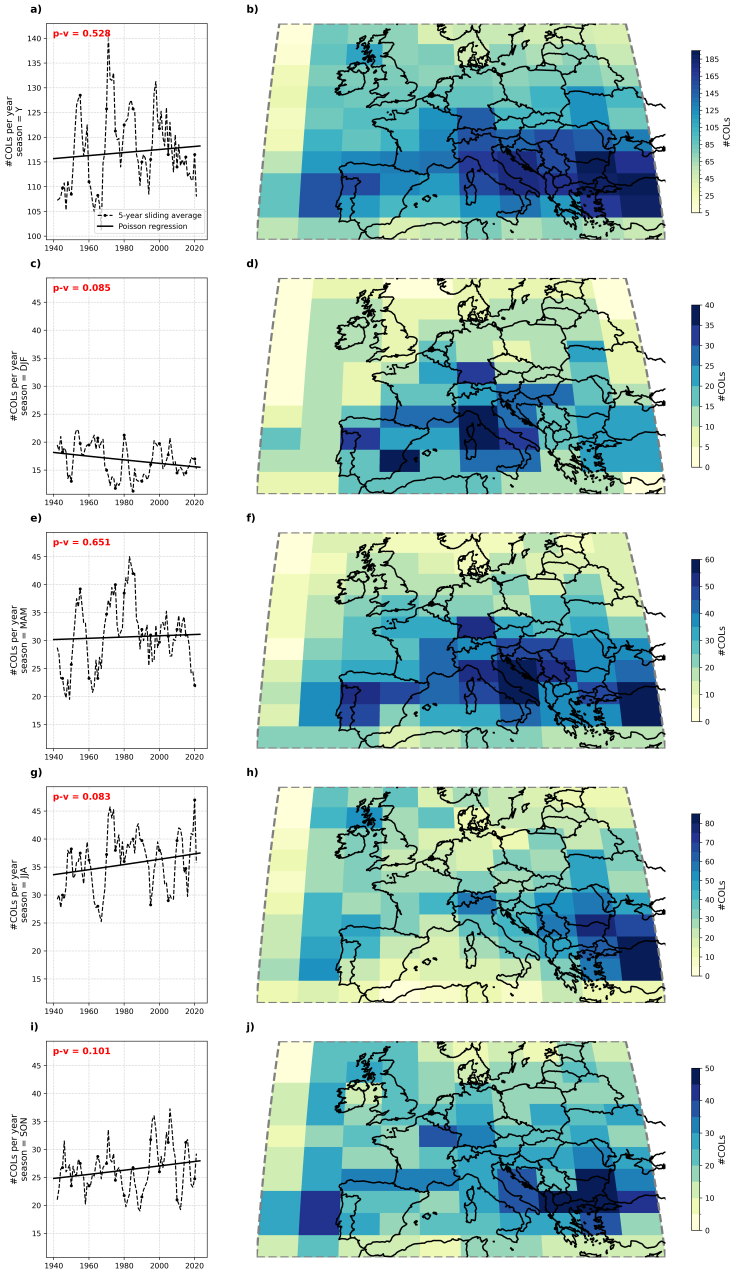

Figure A2. Same as Fig. A1, but with $A_{\mathrm{crit}} = 10^6\,\mathrm{km}^2$.

https://doi.org/10.5194/egusphere-2026-2315
Preprint. Discussion started: 20 May 2026

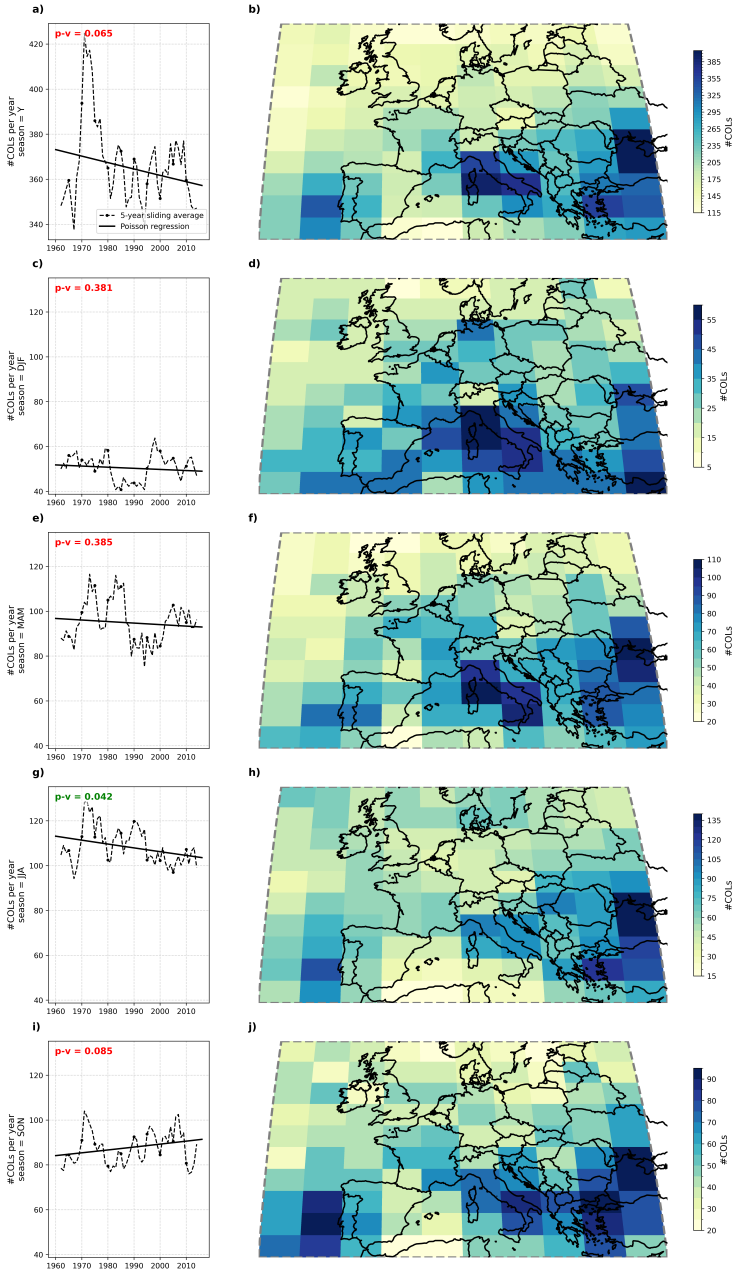

Figure A3. Same as Fig. A1, but over 1960–2017.

https://doi.org/10.5194/egusphere-2026-2315
Preprint. Discussion started: 20 May 2026

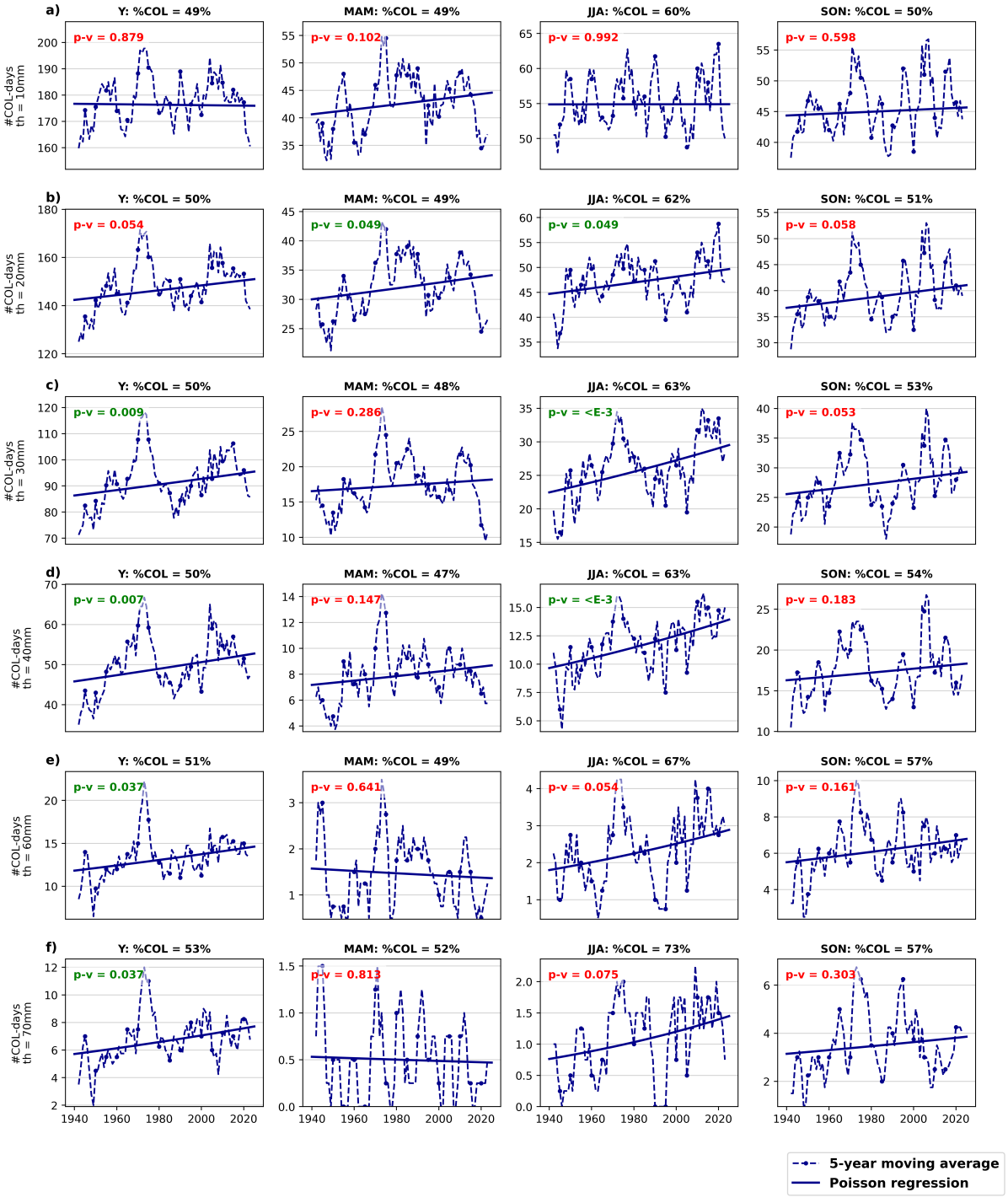

Figure A4. Same as Figure 5of the original paper, but with different precipitation thresholds (a–f).

https://doi.org/10.5194/egusphere-2026-2315
Preprint. Discussion started: 20 May 2026

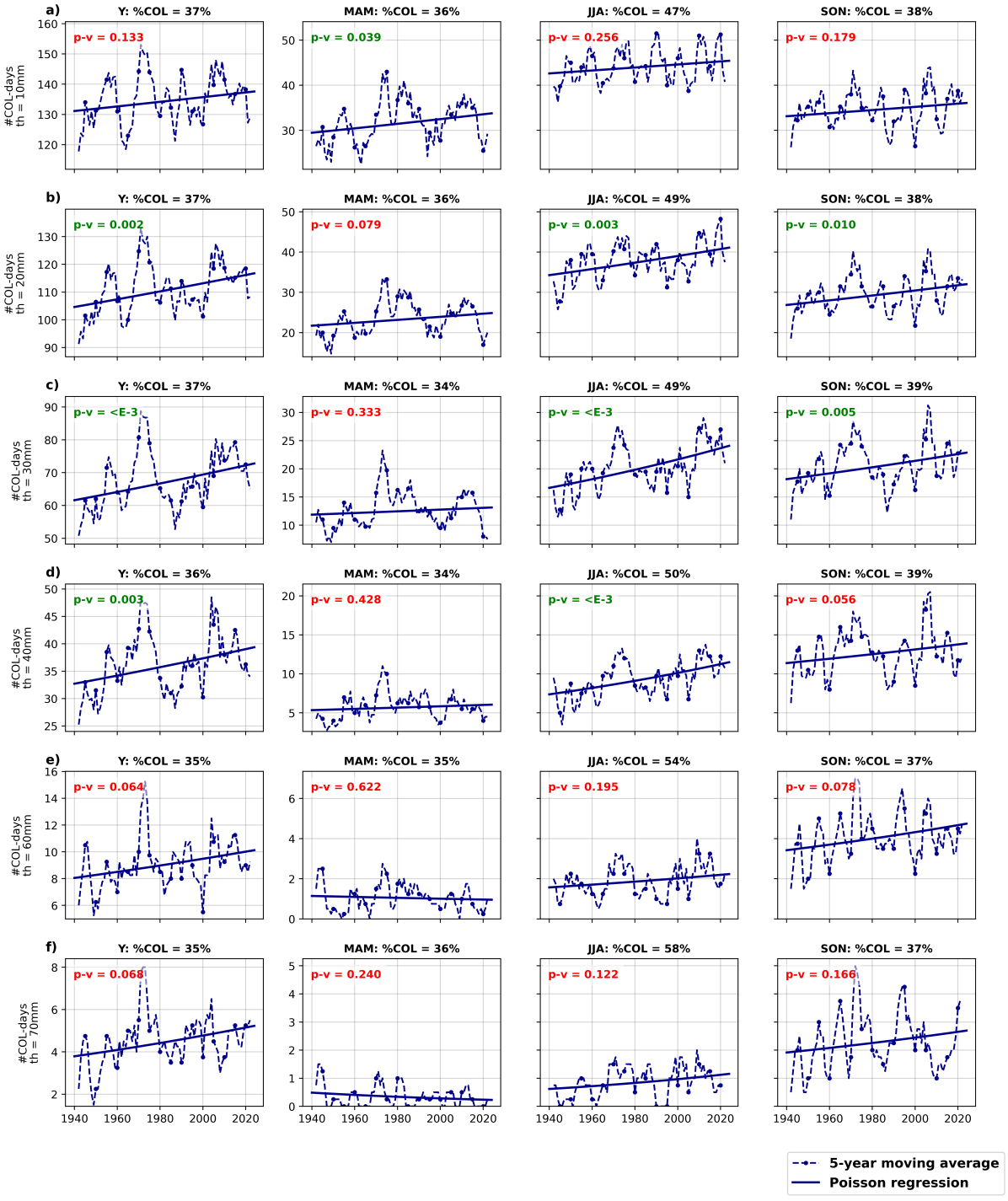

Figure A5. Same as Fig. A4, but with $q_{\text{rain}} = 99$

https://doi.org/10.5194/egusphere-2026-2315
Preprint. Discussion started: 20 May 2026

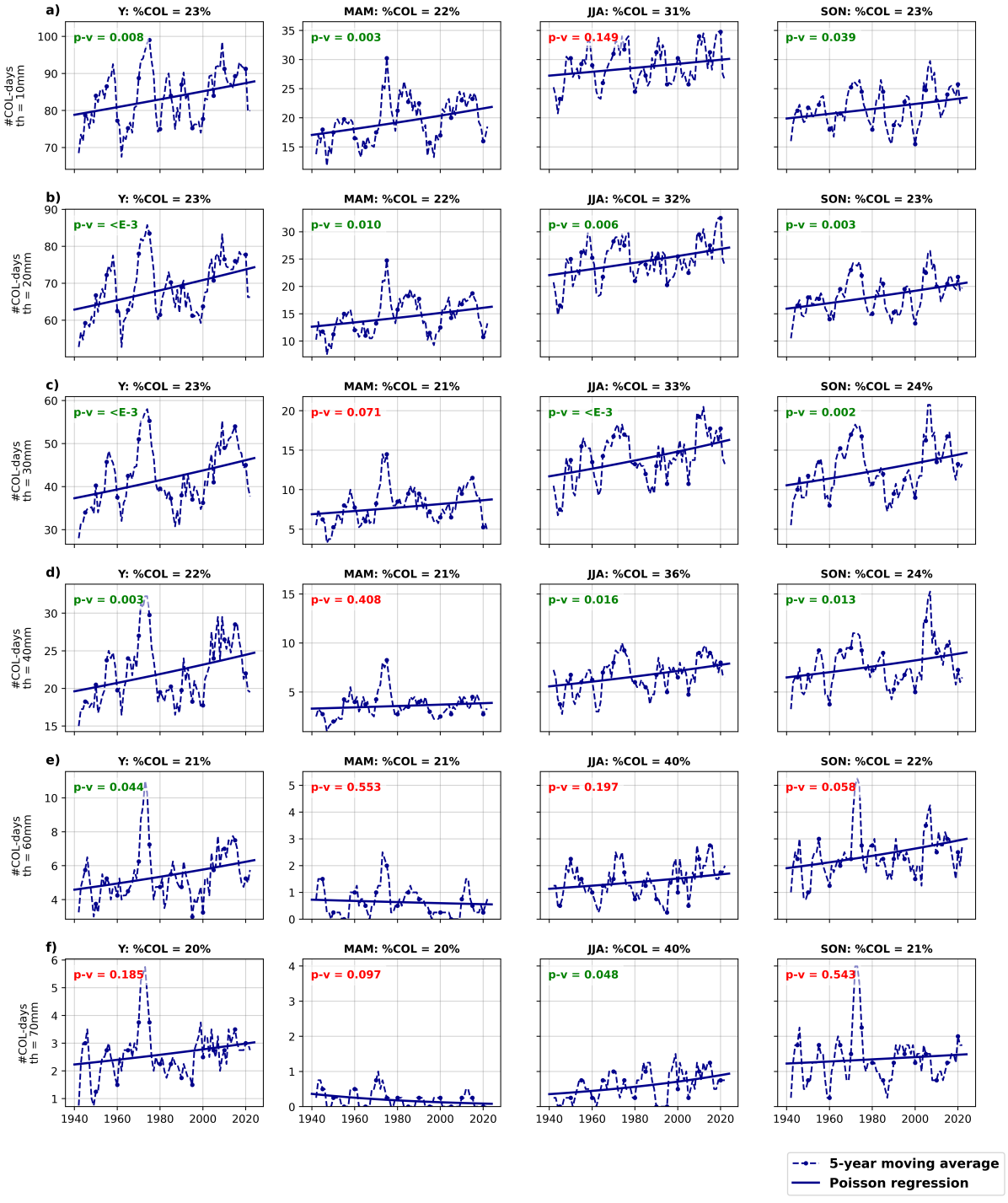

Figure A6. Same as Fig. A4, but with $q_{\text{rain}} = 99.9$

https://doi.org/10.5194/egusphere-2026-2315
Preprint. Discussion started: 20 May 2026

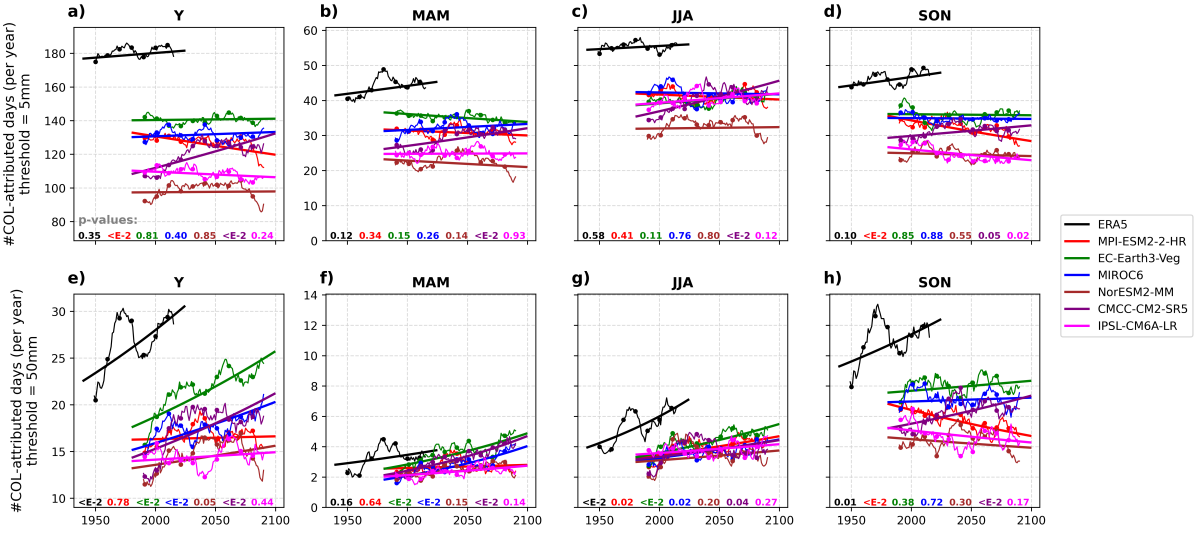

Figure A7. Same as Figure 8 of the original paper, but with the scenario SSP1-2.6.

References

Barnes, M. A., King, M., Reeder, M., and Jakob, C.: The dynamics of slow-moving coherent cyclonic potential vorticity anomalies and their links to heavy rainfall over the eastern seaboard of Australia, Quarterly Journal of the Royal Meteorological Society, 149, 2233–2251, https://doi.org/10.1002/qj.4503, 2023.

Brajkovic, J., Fettweis, X., Noël, B., Vyver, H. V. D., Ghilain, N., Archambeau, P., Pirotton, M., and Doutreloup, S.: Increased intensity and frequency of extreme precipitation events in Belgium as simulated by the regional climate model MAR, Journal of Hydrology: Regional Studies, 59, 102 399, https://doi.org/10.1016/j.ejrh.2025.102399, 2025.

Calvo-Sancho, C., Díaz-Fernández, J., González-Alemán, J. J., Halifa-Marín, A., Miglietta, M. M., Azorín-Molina, C., Prein, A. F., Montoro-Mendoza, A., Bolgiani, P., Morata, A., and Martín, M. L.: Human-induced climate change amplification on storm dynamics in Valencia's 2024 catastrophic flash flood, Nature Communications, 17, 1492, https://doi.org/10.1038/s41467-026-68929-9, 2026.

Coppola, E., Nogherotto, R., Ciarlo', J. M., Giorgi, F., van Meijgaard, E., Kadygrov, N., Iles, C., Corre, L., Sandstad, M., Somot, S., Nabat, P., Vautard, R., Levavasseur, G., Schwingshackl, C., Sillmann, J., Kjellström, E., Nikulin, G., Aalbers, E., Lenderink, G., Christensen, O. B., Boberg, F., Sørland, S. L., Demory, M.-E., Bülow, K., Teichmann, C., Warrach-Sagi, K., and Wulfmeyer, V.: Assessment of the European Climate Projections as Simulated by the Large EURO-CORDEX Regional and Global Climate Model Ensemble, Journal of Geophysical Research: Atmospheres, 126, https://doi.org/10.1029/2019jd032356, 2021.

Dai, T., Dong, W., Yan, G., Zhu, X., et al.: Understanding the Abrupt Climate Change in the Mid-1970s from a Phase-Space Transform Perspective, Journal of Applied Meteorology and Climatology, 57, 2573–2591, https://doi.org/10.1175/JAMC-D-17-0345.1, 2018.

Dewals, B., Erpicum, S., Pirotton, M., and Archambeau, P.: Extreme floods in Belgium: The July 2021 extreme floods in the Belgian part of the Meuse basin, Hydrolink, p. 104, https://hdl.handle.net/20.500.11970/109527, issue 2021/4, 2021.

ECMWF: Storm Boris and European flooding September 2024, https://www.ecmwf.int/en/about/media-centre/focus/2024/storm-boris-and-european-flooding-september-2024, accessed: 2026-03-21, 2024.

https://doi.org/10.5194/egusphere-2026-2315
Preprint. Discussion started: 20 May 2026

Eumetsat: Identifying Cut-off Lows, https://user.eumetsat.int/resources/case-studies/identifying-cut-off-lows, accessed: 2026-03-21, 2024.

Fernández-Alvarez, J. C., Pérez-Alarcón, A., Eiras-Barca, J., Rahimi, S., Nieto, R., and Gimeno, L.: Projected changes in atmospheric moisture transport contributions associated with climate warming in the North Atlantic, Nature Communications, 14, 6476, https://doi.org/10.1038/s41467-023-41915-1, 2023.

Ferreira, R. N.: Cut-Off Lows and Extreme Precipitation in Eastern Spain: Current and Future Climate, Atmosphere, 12, https://doi.org/10.3390/atmos12070835, 2021.

Grandry, M., Gailliez, S., Brostaux, Y., and Degré, A.: Looking at trends in high flows at a local scale: The case study of Wallonia (Belgium), Journal of Hydrology: Regional Studies, 31, 100 729, https://doi.org/https://doi.org/10.1016/j.ejrh.2020.100729, 2020.

Hersbach, H., Bell, B., Berrisford, P., Hirahara, S., Horányi, A., Muñoz-Sabater, J., Nicolas, J., Peubey, C., Radu, R., Schepers, D., Simmons, A., Soci, C., Abdalla, S., Abellan, A., Alonso-Balmaseda, M., Ana, G., and ...: The ERA5 global reanalysis, Quarterly Journal of the Royal Meteorological Society, 146, 1999–2049, https://doi.org/10.1002/qj.3803, 2020.

Hundhausen, M., Feldmann, H., Kohlhepp, R., and Pinto, J. G.: Climate change signals of extreme precipitation return levels for Germany in a transient convection-permitting simulation ensemble, International Journal of Climatology, 44, 1454–1471, https://doi.org/https://doi.org/10.1002/joc.8393, 2024.

Insua-Costa, D., Senande-Rivera, M., Llasat, M. C., and Miguez-Macho, G.: The central role of forests in the 2021 European floods, Environmental Research Letters, 17, 064 053, https://doi.org/10.1088/1748-9326/ac6f6b, 2022.

IPCC: Global Carbon and Other Biogeochemical Cycles and Feedbacks, chap. 5, p. 673–816, Cambridge University Press, 2023.

Jain, S., Scaife, A., Shepherd, T., Deser, C., Dunstone, N., Schmidt, G., Trenberth, K., and Turkington, T.: Importance of internal variability for climate model assessment, npj Climate and Atmospheric Science, 6, https://doi.org/10.1038/s41612-023-00389-0, 2023.

Kendon, E. J., Fischer, E. M., and Short, C. J.: Variability conceals emerging trend in 100yr projections of UK local hourly rainfall extremes, Nature Communications, 14, 1217, https://doi.org/10.1038/s41467-023-36499-9, 2023.

Kreienkamp, F., Philip, S. Y., Tradowsky, J. S., Kew, S. F., Lorenz, P., Arrighi, J., Belleflamme, A., Bettmann, T., Caluwaerts, S., Chan, S. C., Ciavarella, A., De Cruz, L., de Vries, H., Demuth, N., Ferrone, A., Fischer, r. M., Fowler, H. J., Goergen, K., Heinrich, D., Henrichs, Y., Lenderink, G., Kaspar, F., Nilson, E., Otto, F. E. L., Ragone, F., Seneviratne, S. I., Singh, R. K., Skålevåg, A., Termonia, P., Thalheimer, L., van Aalst, M., Van den Bergh, J., Van de Vyver, H., Vannitsem, S., van Oldenborgh, G. J., Van Schaeybroeck, B., Vautard, R., Vonk, D., and Wanders, N.: Rapid attribution of heavy rainfall events leading to the severe flooding in Western Europe during July 2021, 2021.

Ludwig, P., Ehmele, F., Franca, M. J., Mohr, S., Caldas-Alvarez, A., Daniell, J. E., Ehret, U., Feldmann, H., Hundhausen, M., Knippertz, P., Küpfer, K., Kunz, M., Mühr, B., Pinto, J. G., Quinting, J., Schäfer, A. M., Seidel, F., and Wisotzky, C.: A multi-disciplinary analysis of the exceptional flood event of July 2021 in central Europe – Part 2: Historical context and relation to climate change, Natural Hazards and Earth System Sciences, 23, 1287–1311, https://doi.org/10.5194/nhess-23-1287-2023, 2023.

Mishra, A. N., Maraun, D., Schiemann, R., Hodges, K., Zappa, G., and Ossó, A.: Long-lasting intense cut-off lows to become more frequent in the Northern Hemisphere, Communications Earth & Environment, 6, https://doi.org/10.1038/s43247-025-02078-7, 2025.

Moustakis, Y., Onof, C. J., and Paschalis, A.: Atmospheric convection, dynamics and topography shape the scaling pattern of hourly rainfall extremes with temperature globally, Communications Earth & Environment, 1, 3, https://doi.org/10.1038/s43247-020-0003-0, 2020.

Muñoz, C., Schultz, D., and Vaughan, G.: A Midlatitude Climatology and Interannual Variability of 200- and 500-hPa Cut-Off Lows, Journal of Climate, 33, 2201–2222, https://doi.org/10.1175/jcli-d-19-0497.1, 2020.

Pfahl, S., O'Gorman, P. A., and Fischer, E. M.: Understanding the regional pattern of projected future changes in extreme precipitation, Nature Climate Change, 7, 423–427, https://doi.org/10.1038/nclimate3287, 2017.

https://doi.org/10.5194/egusphere-2026-2315
Preprint. Discussion started: 20 May 2026

Pierce, D. W., Cayan, D. R., Maurer, E. P., Abatzoglou, J. T., and Hegewisch, K. C.: Improved Bias Correction Techniques for Hydrological Simulations of Climate Change, Journal of Hydrometeorology, 16, 2421 – 2442, https://doi.org/10.1175/JHM-D-14-0236.1, 2015.

Rajczak, J. and Schär, C.: Projections of Future Precipitation Extremes Over Europe: A Multimodel Assessment of Climate Simulations, Journal of Geophysical Research: Atmospheres, 122, 10,773–10,800, https://doi.org/https://doi.org/10.1002/2017JD027176, 2017.

Rodero Astaburuaga, C.: Valencia's DANA of October 2024: The 12 days of the state of emergency in the province of Valencia (Spain), Spanish Journal of Legal Medicine, 51, 500 457, https://doi.org/https://doi.org/10.1016/j.remle.2025.500457, 2025.

Sarkar, S. and Maity, R.: Global climate shift in 1970s causes a significant worldwide increase in precipitation extremes, Scientific Reports, 11, 11 574, https://doi.org/10.1038/s41598-021-90854-8, 2021.

Schoofs, J., Vandelanotte, K., Van de Vyver, H., Van Der Sichel, L., Vandersteene, M., Serras, F., van Lipzig, N. P. M., and Van Schaeybroeck, B.: Dynamic and thermodynamic contributions to future extreme-rainfall intensification: a case study for Belgium, https://doi.org/10.48550/ARXIV.2502.02436, 2025.

Sobolowski, S., Somot, S., Fernández, J., Evin, G., Brands, S. F., Maraun, D., Kotlarski, S., Jury, M., Benestad, R. E., Teichmann, C., Christensen, O. B., Bülow, K., Buonomo, E., Katragkou, E., Steger, C., Sørland, S., Nikulin, G., McSweeney, C., Dobler, A., Palmer, T., Wilcke, R., Boé, J., Brunner, L., Ribes, A., Qasmi, S., Nabat, P., Sevault, F., and Oudar, T.: GCM Selection and Ensemble Design: Best Practices and Recommendations from the EURO-CORDEX Community, Bulletin of the American Meteorological Society, 106, E1834–E1850, https://doi.org/10.1175/BAMS-D-23-0189.1, 2025.

Tamarin, T. and Kaspi, Y.: The poleward shift of storm tracks under global warming: A Lagrangian perspective, Geophysical Research Letters, 44, https://doi.org/10.1002/2017gl073633, 2017.

Thompson, V., Coumou, D., Galfi, V. M., Happé, T., Kew, S., Pinto, I., Philip, S., de Vries, H., and van der Wiel, K.: Changing dynamics of Western European summertime cut-off lows: A case study of the July 2021 flood event, Atmospheric Science Letters, 25, https://doi.org/10.1002/asl.1260, 2024.

Thompson, V., Coumou, D., Beyerle, U., Ommer, J., Cloke, H. L., and Fischer, E.: Alternative rainfall storylines for the Western European July 2021 floods from ensemble boosting, Communications Earth & Environment, 6, 427, https://doi.org/10.1038/s43247-025-02386-y, 2025.

Tramblay, Y., Neppel, L., Carreau, J., and Najib, K.: Non-stationary frequency analysis of heavy rainfall events in southern France, Hydrological Sciences Journal, 58, 280–294, https://doi.org/10.1080/02626667.2012.754988, 2013.